


Review

# Recent Advances in Nucleic Acid Modulation for Functional Nanozyme

Xin Wang <sup>1</sup>, Yuancong Xu <sup>2</sup>, Nan Cheng <sup>1,\*</sup> , Xinxian Wang <sup>1</sup>, Kunlun Huang <sup>1,3</sup> and Yunbo Luo <sup>1,3,\*</sup>

<sup>1</sup> Beijing Laboratory for Food Quality and Safety, College of Food Science and Nutritional Engineering, China Agricultural University, Beijing 100083, China; b20193060546@cau.edu.cn (X.W.); S20193060998@cau.edu.cn (X.W.); hkl009@163.com (K.H.)

<sup>2</sup> Beijing Key Laboratory of Environmental and Viral Oncology, College of Life Science and Bioengineering, Beijing University of Technology, Beijing 100124, China; xuyuancong@bjut.edu.cn

<sup>3</sup> Key Laboratory of Safety Assessment of Genetically Modified Organism (Food Safety), Ministry of Agriculture, Beijing 100083, China

\* Correspondence: chengnanFSNE@cau.edu.cn (N.C.); lyb@cau.edu.cn (Y.L.); Tel.: +86-010-62737751 (N.C.); +86-010-62736479 (Y.L.)

**Abstract:** Nanozymes have the potential to replace natural enzymes, so they are widely used in energy conversion technologies such as biosensors and signal transduction (converting biological signals of a target into optical, electrical, or metabolic signals). The participation of nucleic acids leads nanozymes to produce richer interface effects and gives energy conversion events more attractive characteristics, creating what are called “functional nanozymes”. Since different nanozymes have different internal structures and external morphological characteristics, functional modulation needs to be compatible with these properties, and attention needs to be paid to the influence of nucleic acids on nanozyme activity. In this review, “functional nanozymes” are divided into three categories, (nanozyme precursor ion)/ (nucleic acid) self-assembly, nanozyme-nucleic acid irreversible binding, and nanozyme-nucleic acid reversible binding, and the effects of nucleic acids on modulation principles are summarized. Then, the latest developments of nucleic acid-modulated nanozymes are reviewed in terms of their use in energy conversion technology, and their conversion mechanisms are critically discussed. Finally, we outline the advantages and limitations of “functional nanozymes” and discuss the future development prospects and challenges in this field.

**Keywords:** nanozyme; nucleic acid; modulation; recognition; energy conversion; interface effect



**Citation:** Wang, X.; Xu, Y.; Cheng, N.; Wang, X.; Huang, K.; Luo, Y. Recent Advances in Nucleic Acid Modulation for Functional Nanozyme. *Catalysts* **2021**, *11*, 638. <https://doi.org/10.3390/catal11050638>

Academic Editor: Gloria Fernandez-Lorente

Received: 24 April 2021  
Accepted: 12 May 2021  
Published: 17 May 2021

**Publisher's Note:** MDPI stays neutral with regard to jurisdictional claims in published maps and institutional affiliations.



**Copyright:** © 2021 by the authors. Licensee MDPI, Basel, Switzerland. This article is an open access article distributed under the terms and conditions of the Creative Commons Attribution (CC BY) license (<https://creativecommons.org/licenses/by/4.0/>).

## 1. From “Enzyme” to “Nucleic Acid Modulation for Functional Nanozyme”

### 1.1. Enzyme

In the field of biology, enzymes are a class of macromolecular substances with biocatalytic functions. Only under suitable temperature and acid-base conditions can enzymes change the physiological state of organisms by regulating their metabolic pathways, such as by signal transduction, gene expression, gene silencing, etc., or by obtaining new biological traits or removing certain biological traits [1,2]. Enzymes usually exhibit excellent catalytic efficiency and regio- and stereoselectivity, and they are widely used in biochemical energy conversion, playing an important role in food risk-factor detection, medical disease diagnosis and treatment, and environmental pollutant analysis [3,4].

Most natural enzymes are proteins or RNA, and some studies have pointed out that enzymes can also be DNA. Natural enzymes lose their activity when encountering nonphysiological conditions, and the preparation process of enzymes is complicated and expensive [5,6]. Therefore, in the past few decades, scientists have been seeking to synthesize compounds with properties similar to enzymes' activity by chemical or physical methods. These compounds are stable, economical, and able to adapt to nonphysiological conditions to solve problems in practical applications [7,8].

## 1.2. Nanozyme

In recent years, nanoparticles (NPs) with strong tolerance to the external environment have shown dual characteristics, including biological properties and material chemical properties, and these NPs are called “nanozymes”, which are expected to replace natural enzymes [9,10]. In 2004, self-assembly triazacyclonane-functionalized thiols on the surface of gold NPs exhibited RNase-like behavior that catalyzed the cleavage of phosphate esters [11]. Then, to define this layer of gold nanoclusters, scientists proposed the concept of a “nanozyme”. NPs with enzymatic activity were later described as nanozymes [12,13]. In 2007, Yan et al. reported for the first time that Fe<sub>3</sub>O<sub>4</sub> nanoparticle (NP) catalysts showed properties similar to peroxidase [14]. The publication of this work changed the traditional concept of inorganic nanomaterials being biologically inert substances, revealed the inherent biological effects and new characteristics of nanomaterials, and expanded from organic composites to inorganic nanomaterials, which broke the boundary between “inorganic” and “organic” in the traditional sense.

Moreover, by combining excellent physical and chemical properties with enzyme-like catalytic activity, nanozymes can realize multifunctional biological applications from detection to monitoring and treatment and have been widely studied in the fields of medicine, chemistry, food, agriculture, and environment [15]. Compared with natural enzymes, nanozymes have the following characteristics [15]:

(1) High stability: Inorganic nanomaterials are more adaptable to pH and temperature changes than natural enzymes. Some nanozyme can be used under a wide range of pH (3–12) and temperature (4–90 °C) conditions. In contrast, biological enzymes are usually easily denatured and inactivated under extreme pH and temperature conditions.

(2) Low cost: The production process of enzymes is usually complicated and expensive, while inorganic nanomaterials are easy to produce on a large scale with good catalytic activity and low cost.

(3) Recycling: Inorganic nanomaterials are recyclable, and there is no significant loss of catalytic activity in the subsequent cycles.

(4) Easy to be multifunctional: nanozymes have a large specific surface area and high surface energy and can be combined with multiple ligands to achieve multifunctionality [16–19].

Nanozymes, as new stars in science, not only have the characteristics of materials chemistry, including a large specific surface area, rich surface morphology, easy modification, and unique size and shape, but also have more attractive biological characteristics, including the ability to respond to physiological reactions and to catalyze biochemical reactions [20–26].

## 1.3. Functional Nanozyme

Due to the excellent dual properties of nanozymes, some specific studies have shown that they can respond well to the changes of biological macromolecules (proteins, nucleic acids, polysaccharides, lipids).

(1) As for proteins, Zhang et al. [27] encapsulated transition metal catalysts (TMCs) on the single-layer surface of gold nanoparticles to prepare a bio-orthogonal nanozyme. By weakening the formation of a constant protein crown (hard corona), the long-term retention of nanozyme activity in the cell is achieved.

(2) As for nucleic acids, Wang et al. [28] found that ssDNA adsorbed on g-C<sub>3</sub>N<sub>4</sub> NSs could improve the catalytic activity of the nanosheets.

(3) As for polysaccharides, Li et al. [29] synthesized soluble molecularly imprinted nanozyme that can accurately hydrolyze the oligosaccharide maltohexaose.

(4) As for lipids, Zhang et al. [30] reported magnetic nanoparticles (iron oxide nanozyme). After a nanozyme enters the cell, it exerts peroxidase activity in the acidic environment of the lysosome, increases the level of ROS activity, destroys proteins, nucleic acids, lipids, and other biological molecules, makes them lose their functions, and kills *Escherichia coli*.

Overall, the structure and surface physicochemical properties of a nanozyme determine whether it has the characteristics to cope well with biological macromolecules' changes and thus to produce unique nanobiological effects.

Among these biological macromolecules, nucleic acids have been known for specific self-assembly properties and unique molecular recognition mechanisms [31]. First, the double-stranded structure of nucleic acids has complementarity, and a series of DNA-based nanomaterials can be developed based on this complementarity between strands [32]. Moreover, as a biological recognition molecule, a nucleic acid aptamer is essentially a single-stranded DNA or RNA folded to form a specific secondary and tertiary conformation that then binds to the target molecule with high affinity and specificity [31].

The increasing development of nucleic acid technology has promoted the progress of studies on biochemical energy conversion related to biomacromolecule-modulating nanozymes (energy conversion: the energy generated by the biochemical event is transformed into other forms of energy, such as light energy, electric energy, new biological energy, or new chemical energy) [33–37]. Specifically, nucleobases can provide lone pairs of nitrogen and oxygen electrons, and nucleobases are an important structure of the nucleic acid phosphate backbone. Thus, nucleic acid acts as a multidentate organic ligand, which interfaces with metal ions, metal oxides, metal organic frameworks, and carbon bases of nanozymes, transferring electrons to form functional nanozymes [38–41]. The interaction between functional nanozymes and various interface components was analyzed by generating energy conversion effects (biosensing and signal transduction) [42]. Like target recognition conversion into an optical signal or electrical signal, the probe assembled by gold nanozyme and aptamer AG3 converts the process of specific recognition of murine norovirus into an optical signal [43]; the probe assembled by the gold nanoparticle–graphene oxide hybrid and the respiratory syncytial virus antibody converts the process of specifically recognizing RSV into an optical signal [44]. Like target substance activation conversion into a metabolic signal, Fe<sub>3</sub>O<sub>4</sub> NPs induce AMPK activation and enhance glucose uptake, which has potential effects in diabetes care [45]; organic polymer nanozyme SPNK induces the release of KYNase, which degrades kynurenine (Kyn) [1]. Consequently, it may be true that nanozymes can control immunomodulation. By studying the interface effects of nanozymes in these energy conversion events and analyzing the interactions between various interface components, we further understand functional nanozymes [42].

#### *1.4. Nucleic Acid Modulation for Functional Nanozyme*

Since one of the centerpieces of the biochemical energy conversion mechanism is the interface modulation event, more attention has focused on the strategy of interface modulation for target assay. To the best of our knowledge, this article is the first to analyze and summarize such phenomena. This article pays great attention to the interface modulation of nucleic acids to nanozymes: modification, binding, immobilization, and the resulting major changes in interface components in the structure of nanozymes, which lead to an increase or decrease in enzyme catalytic activity [46–50]. The controllability and accuracy of modulation technology is an important force for promoting the progress of social civilization. To cater to the perfect control of enzyme activity in practical applications, scientists have expended great effort in studying the crosstalk between nanozymes and nucleic acids, which retains the advantages of nucleic acids but does not limit the properties of nanozymes that need to be expressed.

In short, the crosstalk between nucleic acids and nanozymes has attracted widespread attention in recent years. Our work showed that the advantages of nucleic acids can compensate for the shortcomings of nanozymes and can improve the control of catalytic activity. At the same time, the importance of studying the energy conversion mechanisms of “nucleic acid modulated nanozymes” in terms of risk factor detection for food, medical disease diagnosis and treatment, and environmental pollutant analysis was discussed. Therefore, further research should be carried out to expand the applications of nanozymes.

## 2. Crosstalk between Nanozyme and Nucleic Acid

Nucleic acid modulation of nanozymes is a key step in energy conversion events. Studies have shown that nucleic acids can change the size, shape, composition, surface modification, and state of NPs through biological, chemical, and physical effects [51–54]. Here, we scientifically discuss the construction of three types of crosstalk between nanozymes and nucleic acids: (nanozyme precursor ion)/(nucleic acid) self-assembly, nanozyme-nucleic acid irreversible binding, and NP-nucleic acid reversible binding.

### 2.1. Self-Assembly Nanozyme

The rich structural features of nucleic acids endow them with diverse binding capabilities with NPs. Due to the noncovalent interactions that occur during the assembly of NPs and nucleic acids, the assembled nanozymes have new interface effects and exhibit the desired morphology, chemical-physical properties, and stimulus responsiveness.

Here, we summarize the interactions among components. Recent studies have confirmed that the presence of various elements commonly found in nuclein—oxygen and nitrogen [55]. Nitrogen acts as an electron donor, and oxygen provides electron pairs, which can hybridize or covalently coordinate with single or multiple metal ion precursors (Figure 1); therefore, they can controllably modulate the enzyme activity and stability of nanoparticles [56–60]. In addition, Chen et al. [59] introduced nanocarrier mesoporous silica based on the study of noncovalent binding and discovered that the nucleic acid acted on the platinum particle precursor ion to produce a “reversible” masking effect at the active site.

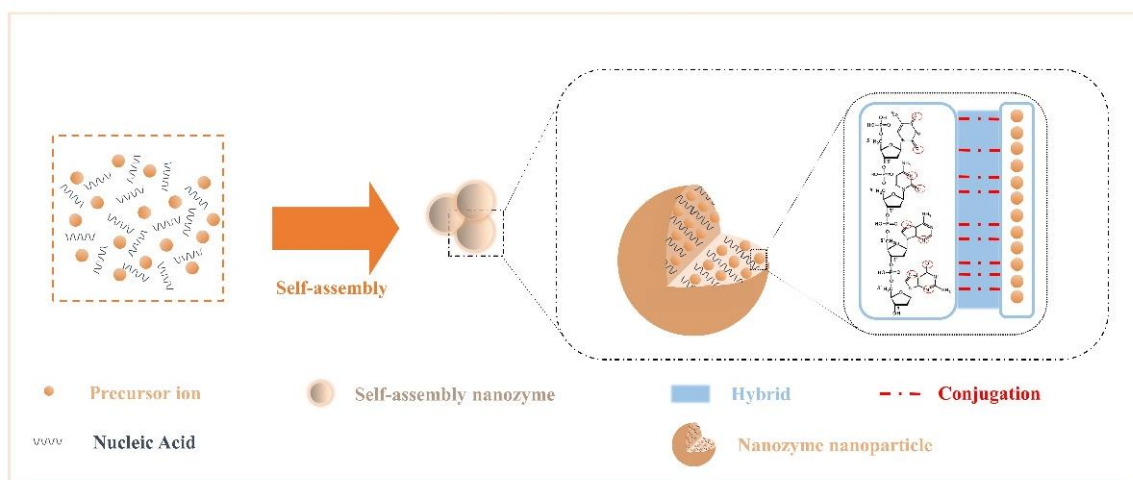


**Figure 1.** Crosstalk from self-assembled nanozymes: noncovalent interactions that occur during the assembly of NPs and nucleic acids.

### 2.2. Irreversible Binding Nanozyme

Nucleic acids have a complex skeletal structure composed of bases, phosphate groups, and ribose, so they have a wealth of modification sites [61,62], while NPs have the characteristics of many surface active sites, strong adsorption, and a high density of valence electrons. Researchers have made use of their rich properties, modified them, and accomplished the irreversible combination of the two components. Many modification bridges have been used to promote binding between NPs and nucleic acids (Figure 2), for example,  $-\text{NH}-\text{SiO}_2-$ ,  $-\text{biotin-streptavidin}-$ ,  $-\text{NH}-\text{COOH}-$ ,  $-\text{C}-\text{NH}-$ ,  $-\text{S}-$ ,  $-\text{magnetic bead}-$ , and  $-\text{NH}-$  [63–69]. Binding at the interface perfectly merges the advantages of the two. Additionally, irreversible chemical modification may affect an NP’s characteristics and limit the number of connections of nucleic acids. In summary, functional nanozymes have both the enzyme activity of NPs and the target recognition function of nucleic acids, producing the desired interface effect, which can be applied to biochemical energy conversion events.

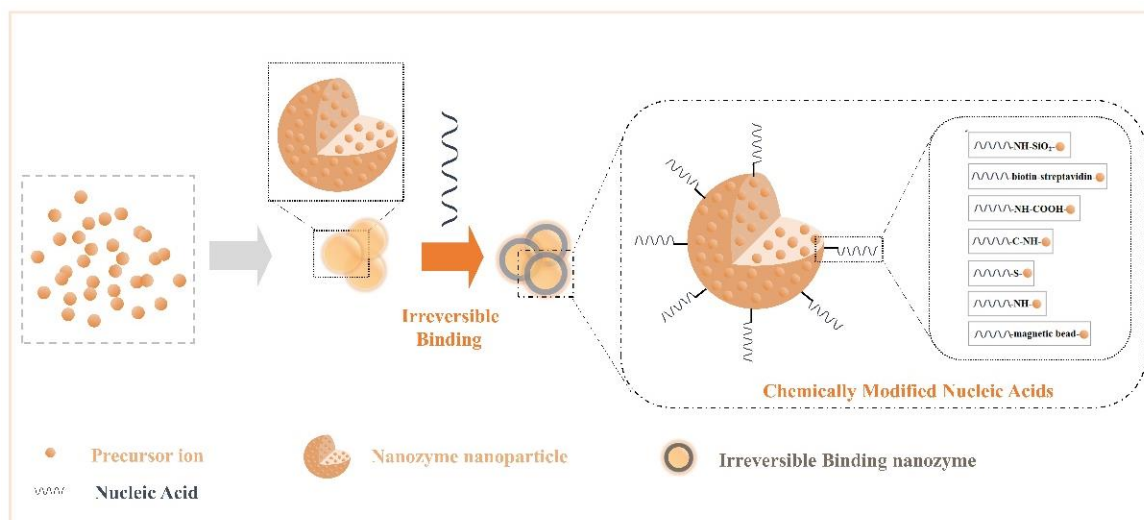


**Figure 2.** Crosstalk from irreversible binding nanozymes: creating irreversible binding nanozymes based on synthetic materials (such as chemically modified nucleic acids).

### 2.3. Reversible Binding Nanozyme

Nucleic acids have parallel stacked bases, polymerized anionic phosphate backbones, sugar rings, and active sites composed of large grooves and small grooves formed by double-stranded structures [26], and these features allow nucleic acids to combine/separate with nanozymes with high specific surface areas and rich surface chemical morphologies, as expected in various analytical events based on competitive binding mechanisms [70]. In general, the addition of nucleic acids to the nanozyme reaction system increases the interface components of the NPs, dramatically increases the free energy of the interface with the NPs, and changes the structure-related properties of the interface, such as ionic valence and electronic transfer. Moreover, it can be formed into a reversible binding nanozyme, which preserves the characteristics of nucleic acids and NP as much as possible. Here, we list the general influence of nucleic acid on NPs (Figure 3) as changes in the steric hindrance effect, changes in the number of active sites, changes in the dispersion of NPs, changes in the structure of NPs (such as oxygen vacancies), and changes in substrate activity in producing highly active substances (such as hydroxyl radicals).

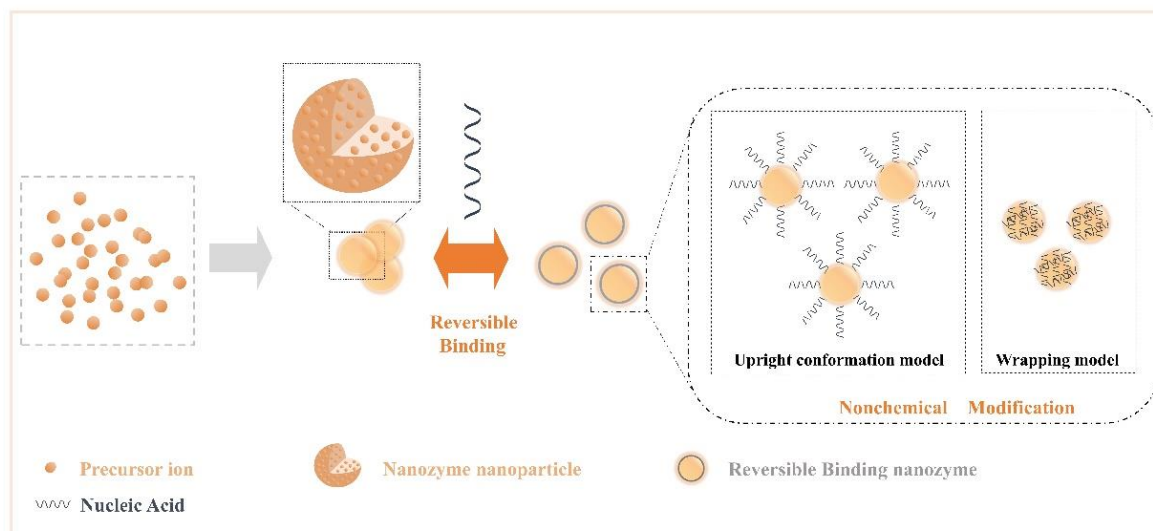


**Figure 3.** Crosstalk from irreversible binding nanozymes and reversible binding nanozymes allow nucleic acids to combine/separate with nanozymes by the effect of intermolecular forces. Reprinted from reference [70].

### 3. Functional Nanozyme-Based Energy Conversion Events

Nucleic acid-modulated nanozymes were studied for energy conversion. First, immobilized indicators, nanozymes, and receptors were required. Second, nucleic acid modulation was required to achieve selective molecular recognition, which was the key to the competitive binding of target substances. Finally, energy conversion events were converted into a variety of optical signals (Figure 4), including changes in light absorption and refraction, fluorescence, chemical or bioluminescence, and Raman scattering [71]. Here, we discuss the energy conversion events from functional nanozymes.

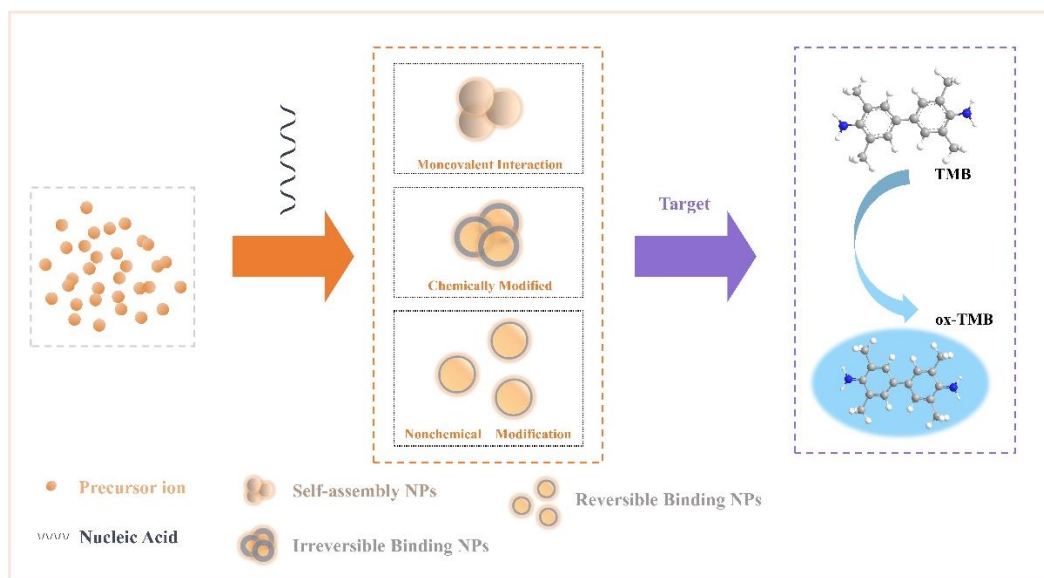


**Figure 4.** Strategy for target assay of functional nanozymes: the interaction between functional nanozymes and various interface components (target, nucleic acid, substrate) was analyzed by generating energy conversion effects (biosensing). Reprinted from reference [71].

#### 3.1. “Self-Assembled Nanozyme”-Based Energy Conversion Events

Nucleic acids with rich and diverse structures are excellent reaction templates for metal ions (metal precursor ions of nanozyme). Due to the noncovalent interaction between the metal precursor ion and nucleic acid, the obtained nanozyme showed controllable morphology, chemical and physical properties, and stimulus responsiveness to achieve more precise positioning and assembly of metal ions nucleic acids [72]. DNA (deoxyribonucleic acid) acted as a template that accurately assembled some metal ions to modulate nanoclusters’ physical and chemical properties, including size, morphology, surface charge, and surface-active sites. These modulations can result in changes in the absorbance, fluorescence intensity, and electromagnetic properties of the nanoclusters [26,72]. Thanks to these excellent modulation capabilities, the precise assembly of metals into nucleic acid nanostructures creates nanozymes that can maintain a metal’s unique properties on the atomic scale. These metal nanozymes, which can easily adjust physicochemical properties by programming nucleic acids, paved a promising way for micro-trace detection and precision medicine. In summary, nanozyme energy conversion not only quantifies recognition events but also amplifies small events.

Nucleic acid modulated single metal precursor ions. Chen et al. [58] developed a method to in situ assemble a DNA-Pt hybrid NP in 7 min. Changing the DNA load can modulate the growth of NPs, the dispersion of NPs, and the surface charge distribution of NPs. The resulting noncovalent bonding and steric hindrance stopped the catalytic activity, which was a highly anticipated phenomenon in sensor analysis events (Figure 5B). Based on these results, a paper-based sensor was developed to achieve rapid quantitative analysis of target nucleic acids with an LOD (limit of detection) as low as 0.228 nM.

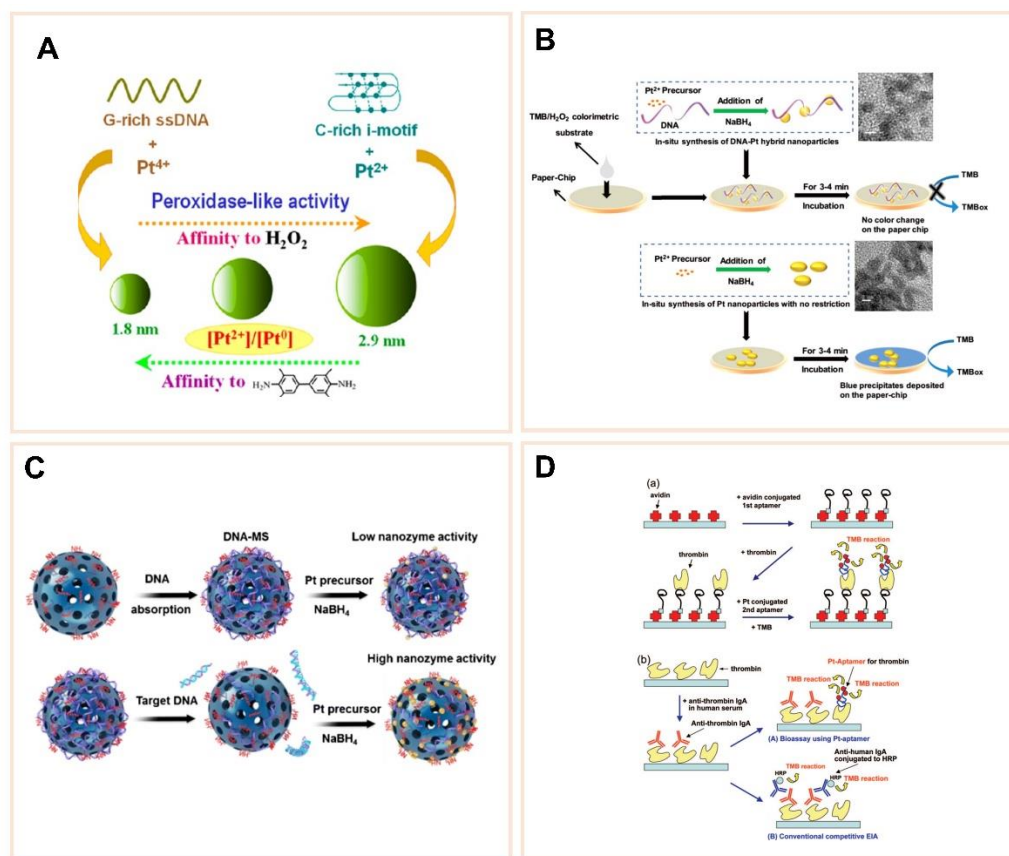


**Figure 5.** “Self-assembled nanozyme”-based energy conversion events: **(A)** Pt NPs synthesized with C-rich sequence i-motif RET2 as the template, initiation of enhanced enzyme activity, conversion of energy into a light signal. Reprinted with permission from reference [56]. Copyright 2014, The American Chemical Society. **(B)** DNA-Pt hybrid NPs. The target nucleic acid recognition process was converted into a weak optical signal. Reprinted with permission from reference [58]. Copyright 2017, Elsevier. **(C)** The nanozyme was formed by ssDNA and platinum precursors deposited on silica (MS) in competition, and the target nucleic acid recognition process was converted into an optical signal. Reprinted with permission from reference [59]. Copyright 2018, Springer Nature. **(D)** Using a thrombin aptamer-Pt nanozyme, the recognition process of thrombin was converted into an optical signal enhancement. Sandwich method of DLAA targeting thrombin **(D-(a))** and competitive DLAA targeting anti-thrombin IgA/G/M **(D-(b))**, **(D-(b)-(A))**, Bioassay using Pt-aptamer, **(D-(b)-(B))**, Conventional competitive EIA. Reprinted with permission from reference [60]. Copyright 2008, The American Chemical Society.

Nonmodified nucleic acid modulated single metal precursor ions. Higuchi et al. [60] synthesized a thrombin aptamer-Pt nanozyme complex through the covalent coordination of lone-pair electrons on the base with Pt<sup>2+</sup>. It was interesting that no functional groups, including biotin, thiol, etc., were used to modify the aptamer, while at the same time, the enzyme-mimicking activity of the NPs was perfectly combined with the specific recognition ability of the aptamer (Figure 5D). Meanwhile, its *K<sub>m</sub>* was comparable with that of hemin-G4 [73–75]. This work led to three conclusions: first, smaller nanozyme complexes had higher enzyme activity; second, enzyme active sites tended to be located on DNA-Pt complexes rather than on independent Pt atoms after coordination; and third, stronger coordination binding forced higher enzyme activity.

Codeposition products come from a hybrid of nucleic acids and a single metal precursor ion. Chen et al. [59] found that single-stranded DNA (ssDNA) and platinum precursors compete to form NPs when deposited on silica (MS). The steric hindrance caused by the competition phenomenon cooperates with the noncovalent force of single stranded DNA

(ssDNA) to combine with the masking effect of the active site of the Pt ion precursor. The precursor active site masking effect achieves the purpose of “turning off” enzyme activity, achieves controllable enzyme activity based on the target nucleic acid, and quickly detects the target based on colorimetric methods (Figure 5C). The linear response of the target concentration of this method is as wide as 5 nM to 100 nM and the LOD is 2.6 nM, and even when there is only one base mismatch, it can be sensitively identified. At the same time, this work found that the complementary sequence can better bind to the target and achieve the purpose of “turning on” enzyme activity. Compatible opening and closing properties are desirable for detecting events and have great potential in practical biochemical energy conversion applications.

Nucleic acids with an i-motif structure modulate a single metal precursor ion. Fu et al. [56] used G- or C-enriched sequences as templates to synthesize Pt nanozymes with particle sizes of 1.7–2.9 nm. Studies have shown that the O atom in cytosine and the N atom in guanine interact with platinum cations, and the binding force of AG22 (G-rich) and Pt<sup>2+</sup> is much higher than that of RET2 (C-rich). The size, morphology, and surface charge distribution of the nanozyme were controlled by adjusting the sequence of nucleic acids and the concentration of Pt<sup>2+</sup> (Figure 5A). In this work, a Pt nanozyme with a Pt<sup>0</sup> content of 66% was synthesized with sequence RET2 of the i-motif structure as a template and showed excellent activity in biochemical energy conversion. The Michaelis–Menten constant (Km) was 0.0560 (using TMB as the substrate), which was higher than that of horseradish peroxidase (HRP) [76].

Based on this research, Sun et al. [57] developed a C-enriched sequence stably loaded bimetallic NP, Au<sub>x</sub>Pt<sub>y</sub> nanozyme, the precursor ion of Au- and Pt-coordinated nucleic acids. When the Pt ratio was 27%, Au<sub>2</sub>Pt<sub>1</sub> was produced, and its Km was 0.088 (using TMB as the substrate), which is similar to that of HRP. Two interface effects from the self-assembled nanozyme were also found. First, DNA prevented coagulation during the bimetallic reduction process. Second, the coordination of nucleobases with Au<sup>+</sup> reduced the ratio of DNA-bound Pt<sup>2+</sup> and simultaneously weakened the inhibitory effect of the bimetallic platinum-based nanozyme activity caused by this reduction. The research used the different forces between nucleic acids and different metals to adjust the enzyme activity and stability of the NPs and enabled multicomponent metals to be stably coreduced, thereby increasing the sulfurophilic function of NPs of different metals.

### 3.2. “Irreversible Binding Nanozyme”-Based Biosensors

The irreversible combination of nucleic acids and nanozymes has rich functions, including high stability of modification performance, target specificity, flexibility of structure conversion, and diversity of interface components, enabling more effective construction of biosensors, which can be used to control enzyme activity and specifically recognize metal ions, small molecules, nucleic acids, and proteins [77–79]. Indeed, such an “Irreversible Binding Nanozyme” system possessed several inherent biosensing superiorities. Firstly, nanozymes have target affinity and recognition ability after chemically modifying nucleic acids. Additionally, nanozymes have the property of catalyzing optical signal enhancement of substrate so that the target can be optically detected by visual inspection. Moreover, the entire detection process does not require hours of molecular extraction or a few days of conventional culture. Here, we briefly list some reports on nanozymes directly modified with nucleic acids.

As shown in Table 1, most of the NPs that directly modify nucleic acids are Fe<sub>3</sub>O<sub>4</sub> nanozymes, which were the first nanozymes discovered, and others are noble metal nanozymes, all of which improve energy conversion efficiency due to the following qualities. First, the encapsulated modified nanozymes show better conversion properties. Hu et al. [63] covalently bound amino-modified nucleic acids to Fe<sub>3</sub>O<sub>4</sub> nanozymes wrapped in SiO<sub>2</sub> and showed that they can specifically recognize proteins and inhibit nanozyme activity through steric hindrance. Target biometrics were transformed into optical signals, and the LOD of thrombin recognition was 0.19 nM (Figure 6a). How-



ever, Zhang et al. [66] coupled an amino-crosslinked chitosan-modified Fe<sub>3</sub>O<sub>4</sub> nanozyme through glutaraldehyde to an aminated thrombin aptamer to specifically capture thrombin, and the thrombin recognition LOD was 1 nM (Figure 6d).

**Table 1.** Information regarding “irreversible binding nanozyme” activity changes used in biosensor research.

Nanozyme	Target	Nucleic Acid	Enzyme Activity Changes	Strategy for Target Assay	LOD	References
Fe <sub>3</sub> O <sub>4</sub>	Thrombin	5'-NH <sub>2</sub> -(CH <sub>2</sub> ) <sub>6</sub> -TTT TTTTTTGGTTGG TGTGGTTG5'-G-3'	Inhibition	Target block the substrate diffusion	0.19 nM	[63]
Fe <sub>3</sub> O <sub>4</sub>	Thrombin	1,5'-biotin-(CH <sub>2</sub> ) <sub>6</sub> -AGT CCGTGGTAGGGCAGG TTGGGGTGACT-3'	Enhancement	Target bound aptamer-nanozyme	1 nM	[66]
Fe <sub>3</sub> O <sub>4</sub>	<i>Streptococcus mutans</i>	5'-biotin-TTTATACTAT CGCATTCTTCCGAG GGGGGGGGGGGGGG GGGGGGGGGGGGGTC GGT-3'	Inhibition	Target block the substrate diffusion	12 CFU/mL	[64]
Fe <sub>3</sub> O <sub>4</sub>	<i>Listeria monocytogenes</i>	5'-NH <sub>2</sub> -TTTTTTTTTTA TCCATGGGGCGGAG ATGAGGGGAGGAG GGCGGTACCCGGTT GAT-3'	Enhancement	Target bound aptamer-nanozyme	5.4 × 10 <sup>3</sup> CFU/mL	[65]
Fe <sub>3</sub> O <sub>4</sub>	Cardiac troponin I	5'-CGCATGCCAAACG TTGCCTCATAGTCCC TCCCGTGTC-3' 5'-biotin-ATAGGAGTC ACGACGACCAGAAA GTAATGCCCGGTAGT	Enhancement	Target bound aptamer-nanozyme	3–10 CFU/mL	[67]
Pt/Pd	<i>Salmonella</i>	TATTCAAAGATGAGT AGGAAAAGATATGT GCGTCTACCTCTTGA CTAAT-3'	Inhibition	Target block the substrate diffusion	3–10 CFU/mL	[68]
Pd	Carcinoembryonic antigen CEA	3'-NH <sub>2</sub> -AGGGGGTG AAGGGATACCC-5'	Enhancement	Target bound aptamer-nanozyme	20 fg/mL	[69]

Second, the functionalized aptamer improved the energy conversion efficiency. For example, Zhang et al. [64] conjugated biotinylated nucleic acids to streptavidin-modified Fe<sub>3</sub>O<sub>4</sub> nanozymes. This work described two types of nucleic acids: nonfunctionalized and G4-hemin functionalized nucleic acid binding aptamers (Figure 6b). Among them, the functionalized enzyme not only increased the specific recognition ability for *Streptococcus mutans* but also enhanced the enzyme activity and recognized a target concentration in saliva as low as 12 CFU/mL. However, Zhang et al. [65] conjugated carboxylated Fe<sub>3</sub>O<sub>4</sub> nanozymes to aminoated nucleic acids and converted the nucleic acid-specific binding events to *Listeria monocytogenes* into a colorimetric signal output (Figure 6c) with a visual limit of 5.4 × 10<sup>3</sup> CFU/mL (Table 1). In another example, Wu et al. [69] used polyhistidine peptides that underwent a Michael addition through cysteine to combine with sulfo-SMCC-ylated G-quadruplex/heme (hCG). Pd nanozymes and carcinoembryonic antigen aptamers (CEA Apt) were combined with toluidine blue. The bioconjugated probe hGQ-peptide/CEA Apt/Pd NPs specifically recognized CEA with femtogram-level sensitivity (Figure 6g). Sun et al. [67] used in situ chemical oxidation polymerization to prepare a Au-PDA-Fe<sub>3</sub>O<sub>4</sub> magnetic nanocomposite, fixed the thiolated G-rich sequence and HRP on the nanocomposite through metal thiol bonds, and then added hemin (Figure 6e). Due to the triple enzymatic activity of the nanomimic enzyme, G4-Hemin, and HRP, recognition of the target cardiac troponin I was possible at the picogram scale. The downside was the complicated functional design of the nucleic acid components, which was not an expected property of the otherwise excellent detection tools.

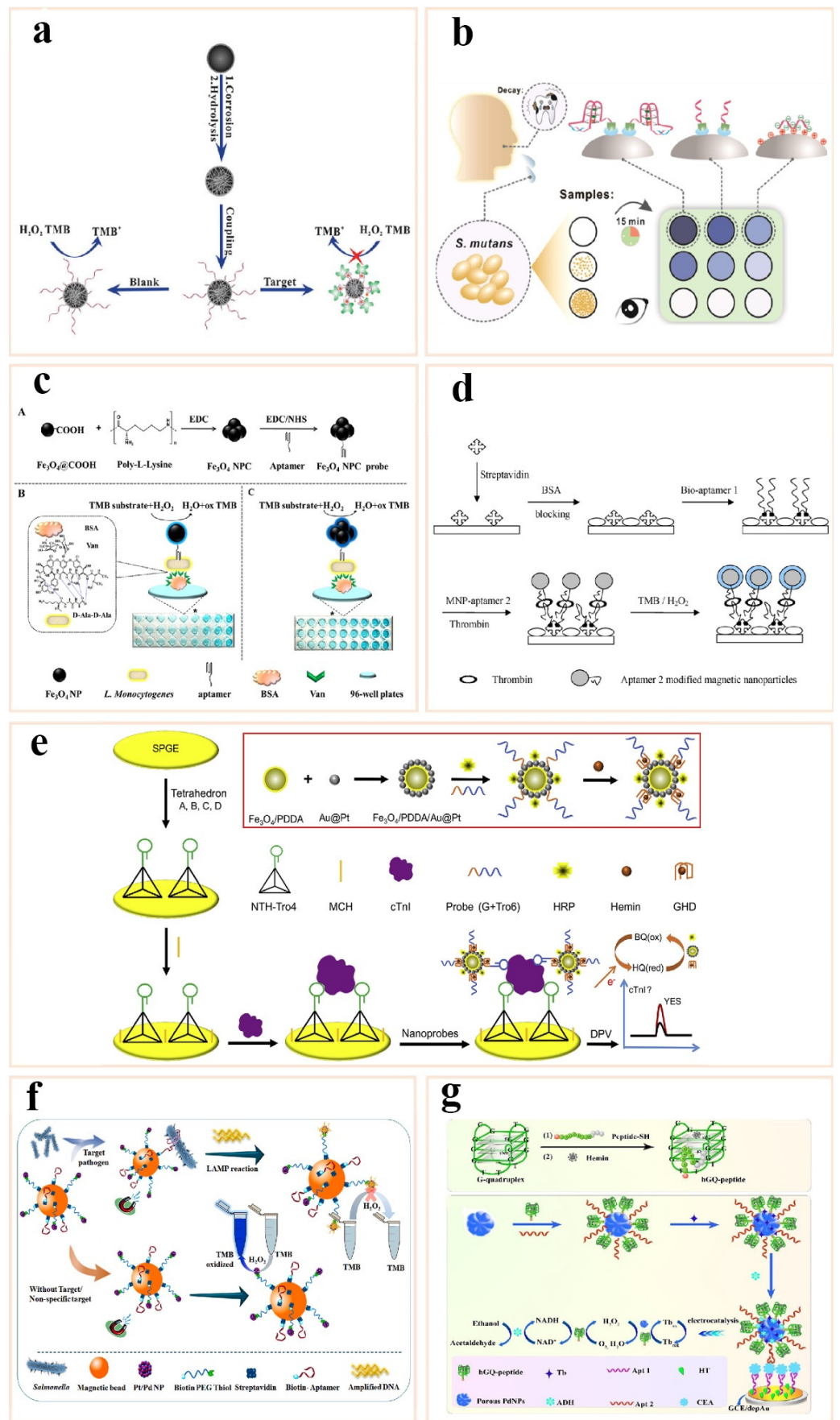


**Figure 6.** “Irreversible binding nanozyme”-based biosensors: (a) An aminated nucleic acid was covalently bound to an  $Fe_3O_4$  nanozyme coated with  $SiO_2$ , and the thrombin recognition process

was converted into an optical signal. Reprinted with permission from reference [63]. Copyright 2013, Royal Society of Chemistry. (b) A biotinylated nucleic acid was conjugated to an Fe<sub>3</sub>O<sub>4</sub> nanozyme modified with streptavidin, and the specific recognition process of *S. mutans* (*Streptococcus mutans*) was converted into a weak optical signal. Reprinted with permission from reference [64]. Copyright 2019, The American Chemical Society. (c) An aminated nucleic acid was conjugated to a carboxylated Fe<sub>3</sub>O<sub>4</sub> nanozyme, which specifically bound to the *L. monocytogenes* (*Listeria monocytogenes*), producing an optical signal. Schematic representation for the preparation of Fe<sub>3</sub>O<sub>4</sub> NPC (c-A), the principle of the Fe<sub>3</sub>O<sub>4</sub> NP-based biosensor (c-B), and the Fe<sub>3</sub>O<sub>4</sub> NPC catalyzed signal amplification biosensor (c-C). Reprinted with permission from reference [65]. Copyright 2016, Elsevier. (d) Fe<sub>3</sub>O<sub>4</sub> nanozymes were coupled to aminated thrombin aptamers via glutaraldehyde, which specifically captured thrombin events and converted them into an optical signal. Reprinted with permission from reference [66]. Copyright 2010, Elsevier. (e) A sequence of the thiolated G-rich aptamer was immobilized on a Au-PDA-Fe<sub>3</sub>O<sub>4</sub> magnetic nanocomposite through metal thiol interactions, and the identified cardiac troponin I event was converted into an optical signal. Reprinted with permission from reference [67]. Copyright 2019, Elsevier. (f) Biotin-modified Pt/Pd nanozymes and nucleic acids were simultaneously immobilized on magnetic beads by streptavidin specifically to capture *Salmonella typhimurium*, and the event was converted into an optical signal. Reprinted with permission from reference [68]. Copyright 2020, Elsevier. (g) A bioconjugated hGQ-peptide/CEA Apt/Pd nanozyme specifically recognized the carcinoembryonic antigen CEA and was converted into an optical signal. Reprinted with permission from reference [69]. Copyright 2018, Elsevier.

Third, the amplification platform was connected through aptamers to amplify the energy conversion efficiency. Zahra et al. [68] simultaneously immobilized biotin-modified Pt/Pd nanozymes and nucleic acids on magnetic beads through streptavidin without enrichment or DNA extraction, directly isolated *Salmonella typhimurium* from food samples, and then amplified DNA using loop-mediated isothermal amplification (Figure 6F). The total analysis time was less than 3 h, and the LOD was 3–10 CFU/mL (Table 1).

### 3.3. “Reversible Binding Nanozyme”-Based Energy Conversion Events

Many NPs can adsorb small molecules and polymers [80,81]. These adsorbed compounds may change the interface between nanozymes and their substrates. Therefore, through adsorption, the catalytic activity of the nanozyme is modulated [82].

The reversible combination of nucleic acids and nanozymes contributes to the modulation of interface effects that help in the analysis of biological energy conversion [83–89]. First, nucleic acid structure not only exhibited a rich conformation but also generated electrostatic forces with the polycation electrolyte due to the phosphate group (anionic polyelectrolyte). Second, single-stranded nucleic acids had chain-like macromolecules, phosphoric acid groups, and aromatic ring-rich structures. These features ensured the reversible affinity of the nucleic acid structure. Subsequently, structural affinity was guaranteed by the effect of intermolecular forces (hydrophobic forces, van der Waals forces, electrostatic forces, hydrogen bonding, aromatic ring stacking, complexation, chelation) [82]. Third, these interaction forces were very interesting because they changed the interface effect, caused the interface components to crosstalk, triggered electron transfer, and converted energy into an optical signal, such as changes in light absorption and refraction, fluorescence, chemical or bioluminescence, and Raman scattering. Additionally, the surface charge of nanozymes can be controlled not only by changing pH but also by adsorbing small molecule anions. Accordingly, these characteristics ensure the application potential of “Reversible Binding Nanozyme” in label-free, transplantable, and visualized targeted detection or therapy. Here, we review and analyze the relevant reports of NP–nucleic acid reversible binding.

### 3.3.1. Physical Properties Changes

Interfacial forces cause changes in the physical properties of interface components, such as steric hindrance/physical barriers, physical adsorption, and dispersion [90–92].

Nucleic acid physically blocked the interaction between the nanozyme and substrates and modulated the biochemical energy conversion. Wang et al. [93] compared the different interface effects between nucleic acids and  $\text{MnO}_2$  and between nucleic acids and GO and found that, unlike nucleic acid adsorption to GO through aromatic ring accumulation and hydrogen bonding forces, nucleic acids bind  $\text{MnO}_2$  through phosphate backbone coordination. The interface between the anionic polyelectrolyte nature of the nucleic acid itself and  $\text{MnO}_2$  generates an electrostatic force, which increases the spatial distance between the substrate and the nanozyme  $\text{MnO}_2$  (steric hindrance) and shuts down the activity of the nanozyme (Figure 7A). Interestingly, after complementary strands were added, these nucleic acids could compete to bind to the single strands on  $\text{MnO}_2$ , which was desirable for biological detection events. In addition,  $\text{MnO}_2$  was dissolved by thiols to release the adsorbed nucleic acid to achieve the detection of glutathione (LOD 383 nM), which cannot be achieved by other metal oxides (such as  $\text{Fe}_3\text{O}_4$ ,  $\text{CeO}_2$ ,  $\text{TiO}_2$ ), and this property can be used in targeted delivery.

This phenomenon agrees with the earlier work of Pautler et al. [82]. On the one hand, nucleic acids coordinated with  $\text{CeO}_2$ , consistent with hard soft acid base theory (HSAB). The nucleic acid played the role of a hard base, and  $\text{CeO}_2$  played the role of a hard acid.  $\text{CeO}_2$  also controlled the surface charge through pH and inorganic anions and generated electrostatic forces with nucleic acids (Figure 7B). The forces of these two phenomena effectively led nucleic acids at concentrations as low as 5  $\mu\text{M}$  to bind tightly to the nanozyme, resulting in a steric hindrance effect, thereby outputting an optical signal that inhibited the activity of the nanozyme. These findings provide meaningful insight into low-concentration nucleic acid modulation of nanozyme-related biochemical energy conversion.

In contrast, nucleic acids physically adsorb both nanozymes and substrates, shorten the spatial distance of interface components, and modulate transduction events. Liu et al. [94] noted that positively charged  $\text{Fe}_3\text{O}_4$  NPs tightly adsorbed to the phosphate backbone of nucleic acids and then assembled into negatively charged NPs. Next, the ssDNA anchored on  $\text{Fe}_3\text{O}_4$  NPs, on the one hand, generated electrostatic forces; on the other hand, the base generated hydrogen bonds and aromatic ring accumulation forces, both of which cooperated to bring the substrate closer to the nanoparticles. Ultimately, the enzyme activity was enhanced. Based on this work [94], Li et al. [95] analyzed the content of ATP in blood with a linear concentration range of 0.50–100  $\mu\text{M}$  (Figure 7C), which can be used to diagnose ATP-indicative diseases [96,97] and is better than most methods that have been reported [98–103].

Overall, compared with other published electrochemical signals, fluorescent signals, and colorimetric signals, nucleic acid-modulated nanozymes caused changes in physical properties and then converted them into an optical signal, which was expected to improve sensitivity.

### 3.3.2. Chemical Properties Changes

Interfacial forces cause changes in the chemical properties of interface components, such as active sites, active products, and reaction activity.

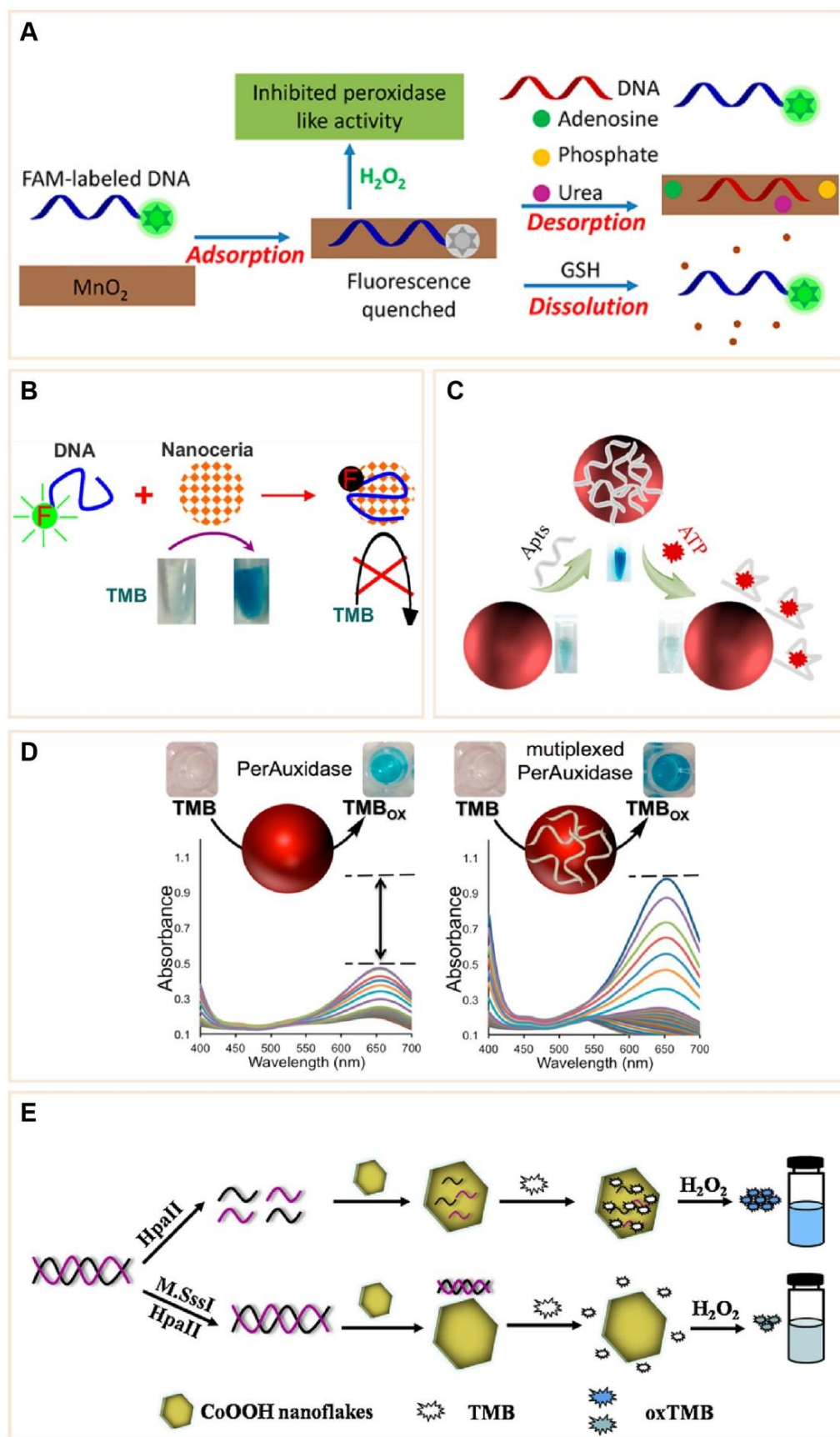


**Figure 7.** For the “reversible binding nanozyme”, the changes in the spatial distance of interface components were used to modulate energy conversion events: (A) An aptamer of glutathione increased the spatial distance between the substrate and nanozyme MnO<sub>2</sub> (steric hindrance effect)

and inhibited enzymatic catalysis, which was converted into a weak optical signal. Reprinted with permission from reference [93]. Copyright 2018, The American Chemical Society. (B) A nucleic acid was tightly bound to the nanozyme, resulting in a steric hindrance effect, inhibition of enzymatic catalysis, and conversion of energy into a weak optical signal. Reprinted with permission from reference [82]. Copyright 2013, The American Chemical Society. (C) The ssDNA anchored on the Fe<sub>3</sub>O<sub>4</sub> nanozyme minimized the distance between the substrate and the NP. The energy change came from the enhancement of enzyme catalysis, and it was converted into a light signal. Reprinted with permission from reference [95]. Copyright 2019, The American Chemical Society. (D) DNA acted on Au NPs to reduce the spatial distance from TMB, enhanced enzyme catalysis, and enhanced the conversion into a light signal. Reprinted with permission from reference [104]. Copyright 2015, The American Chemical Society. (E) DNA acted on the CoOOH nanozyme to reduce the spatial distance with TMB, enhanced enzyme catalysis, and enhanced the conversion into a light signal. Reprinted with permission from reference [105]. Copyright 2018, Elsevier.

Hizir et al. [104] found that when present in pairs as opposed to single bases, different bases expressed different nanozyme activities. Experiments confirmed that nucleobases and Au NPs were combined by hydrogen bonding, and the combined NPs were negatively charged. Moreover, functional NPs shorten the spatial distance from the positively charged substrate TMB through electrostatic forces and hydrogen bonds to enhance enzyme activity (Figure 7D). Li et al. [105] utilized the same mechanism to modulate CoOOH nanozymes (Figure 7E). In their work, the detection limit was 0.069 U/mL for the cancer marker M. Sssl MTase.

The nucleic acids changed the chemical properties of the nanozymes and the substrates and modulated biochemical energy conversion. There are divergent opinions in existing reports on the modulation of CeO<sub>2</sub> NPs by DNA, and it can be said that there are some conflicts [82,91,106]. Dingding et al. [107] selected nanorods, nanocubes, and nanoparticles as research objects to explore the modulation of ssDNA on these three nanozymes with different morphologies. This work produced the following results:

(1) Spatial distance: DNA acted on NPs, causing the surface charge of NPs, the dispersion of CeO<sub>2</sub> NPs, and the spatial distance from the substrate to change. However, the changes in spatial distance were not the main reason for the changes in nanoparticle enzyme activity.

(2) Active site: DNA acted on NPs, causing changes in the Ce<sup>3+</sup> content on the surface of NP. However, the change of Ce<sup>3+</sup> in the active site was not the main reason for the change in NPase activity. Further research, in other reports, showed that DNA acted on the substrate through bases, which was not confirmed in this work [28,94,95,104,105].

The final conclusion of this work was that DNA was coordinated with NP through phosphoric acid groups, which resulted in different exposed crystal faces of NPs with different morphologies, thereby changing the enzyme activity (Figure 8A). Interestingly, although the interaction between the phosphate backbone and nanoparticles was in line with HSAB theory, this study focused on the inherent properties of the material, specifically the three morphologies of NPs and the difference in chelation between the phosphate backbone, which means that the active sites of the three DNA–NPs were different [108–110]. Compared with the research of Pautler et al. [82], which focused on external factors, nucleic acid-wrapped NPs were found to block the contact between NPs and the substrate and to inhibit enzyme activity under physiological conditions.

Here, we found that the nucleic acid concentrations used in the two studies were different (0.5 μM in the study of Dingding [107], 5 μM in the study of Pautler [82]), and the NPs were also different (composition, size, morphology). The morphology [111–114] and size [115–119] of NPs play an important role in catalytic activity. Therefore, it was impossible to compare the two studies in parallel or to objectively speculate that different nucleic acid concentrations will have different effects on NP activity. However, spatial distance and active sites do not always exist in isolation in energy conversion events of the

interaction between nucleic acids and NP; sometimes, they coexist, and one of the factors plays a major role that is more easily observed by researchers.

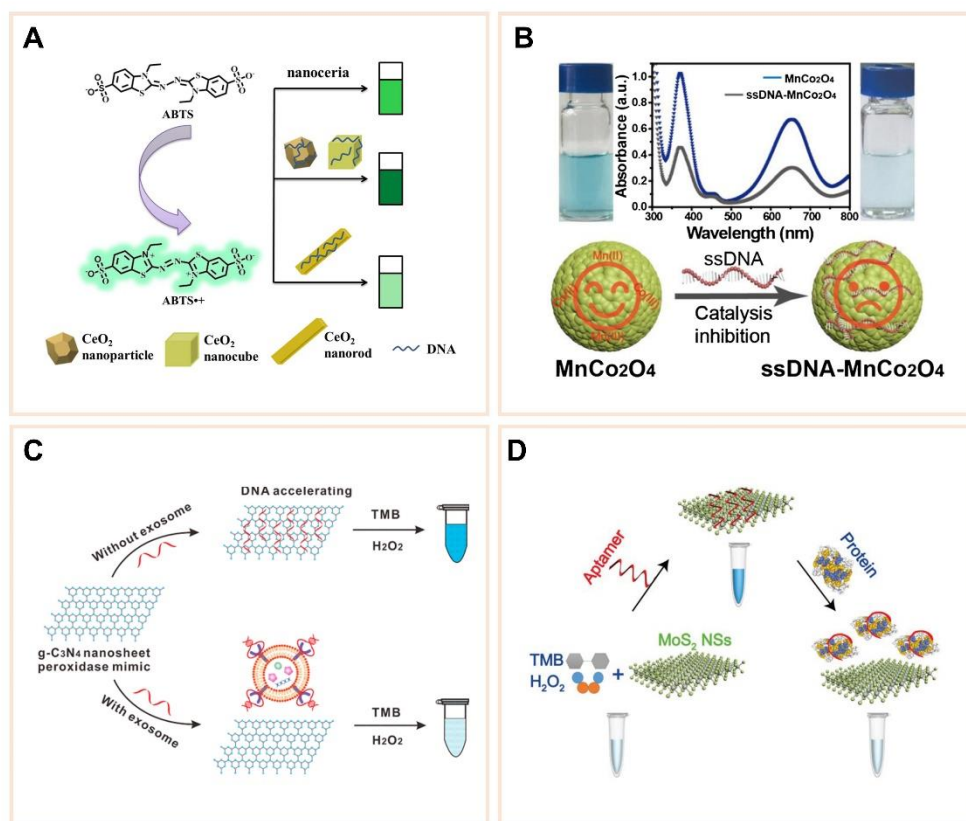


**Figure 8.** For the “reversible binding nanozyme”, the changes in the active sites of the interface components were used to modulate energy conversion events: (A) An interaction occurred between the nucleic acid and NP interface, the active sites exposed by NPs of different morphologies were different, and the energy of the enzyme-catalyzed process was modulated to change the optical signal. Reprinted with permission from reference [107]. Copyright 2018, Institute of Physics. (B) The aptamer shut down the active site of MnCo<sub>2</sub>O<sub>4</sub>, inhibiting the enzymatic process and converting into a weak optical signal. Reprinted with permission from reference [120]. Copyright 2018, Elsevier. (C) Nucleic acid enhanced the ability of the g-C<sub>3</sub>N<sub>4</sub> nanosheet to obtain electrons, increased the number of active sites, and increased the conversion into an optical signal. Reprinted with permission from reference [28]. Copyright 2017, The American Chemical Society. (D) MoS<sub>2</sub> NSs (nanosheets) adsorbed ssDNA, increased the enzyme activity, and enhanced the optical signal. Reprinted with permission from reference [121]. Copyright 2020, Royal Society of Chemistry.

Some studies also focus on the same kind of NP. One modulation mechanism involved the addition of aptamers, which increased the interface components and closed the active sites, thereby inhibiting enzyme activity. Lunjie et al. [120] reported that aptamers reversibly bind MnCo<sub>2</sub>O<sub>4</sub> through electrostatic interactions, thereby switching the oxidase activity of the NP (Figure 8B). The enzymatic activity mechanism of MnCo<sub>2</sub>O<sub>4</sub> includes the formation and elimination of oxygen vacancies (defects left by the escape of oxygen ions from the nanocrystalline lattice), which are the active sites of the NP, and stability (redox cycle), accelerating the electron transfer between NP and substrate TMB.

Another modulation mechanism involved the addition of aptamers, which increased the ingredient in the reaction system and closed the active sites of the NP’s interface, thereby inhibiting enzyme activity. Wang et al. [28] studied the interface force between ssDNA and g-C<sub>3</sub>N<sub>4</sub> nanosheets and made three important findings (Figure 8C). First, ssDNA bound to nanosheets through electrostatic interactions with the aromatic ring of the base. Second,

ssDNA bound to the substrate (TMB) through electrostatic interactions with the aromatic ring and hydrogen bonding with the base. Third, TMB with a conjugated structure was adsorbed on the surface of nanosheets through the accumulation of aromatic rings. As a new interface component, ssDNA affected the interface between the nanosheet and the substrate. ssDNA was multivalently bound to nanosheets, increasing the number of active sites. Additionally, ssDNA has simultaneous affinity for the nanosheets and substrates, shortening the spatial distance and making electron transfer events easier. The reason why this mechanism of modulating enzyme activity was classified based on active site changes was that the aromatic ring structure of the nanosheets had a weak interaction with the substrate, and the addition of nucleic acids produced new interactions with the interface components, breaking the original conjugation between TMB and the nanosheets, increasing the amount of active sites of nanosheets (stronger electron-acquiring ability), and changing the chemical and biological energy at these interfaces. Finally, the colorimetric signal was converted into an output signal. Because of interface modulation, enzyme activity was enhanced by at least a factor of 4. Finally, in the end, the team applied this mechanism to the detection of CD63 exosomes produced by a breast cancer cell line (MCF-7) with a detection limit of  $0.19 \times 10^7$  particles/ $\mu\text{L}$ .

In the same way, Zhao et al. [121] found that after polymer MoS<sub>2</sub> nanosheets adsorbed ssDNA through van der Waals forces, the negative charge of the nanosheets increased, and the electrostatic force between nanosheets and TMB increased (Figure 8D). The interface effect showed that as soon as the activity of the nanosheets increased, the transfer speed of electrons from TMB to H<sub>2</sub>O<sub>2</sub> was accelerated. Because of interface modulation, enzyme activity increased by 4.3 times. The energy change of the interface was shown as an optical signal, which can monitor CEA visually and detect at least 50 ng/mL.

In addition to the above reasons, there was another reason why this mechanism may one day attract greater attention despite it being only indirectly related to these reports. The reason is that the interfacial reactions had not yet been introduced in biological macromolecules, and the appearance of highly active intermediates increased the interface components, making the interfacial reactions more exciting.

It has long been reported that free radicals can promote enzyme activity. Kitajima et al. [122] and Mochida et al. [123] proposed a free radical reaction chain in which Pt NPs trigger the cleavage of O-O bonds to generate highly active hydroxyl radicals, promote H<sub>2</sub>O<sub>2</sub> to obtain electrons, and ultimately promote H<sub>2</sub>O<sub>2</sub> oxidation and decomposition. Ma et al. [124] proposed that based on the free radical chain reaction triggered by accelerated electron transfer, the speed of electron transfer was accelerated, which led to the formation of the catalytic intermediate hydroxyl radical (Figure 9A). Chen et al. [125] further expanded on this research and proposed two points of view. First, PtPd bimetallic nanosheets increase Pt reactivity. Second, the large surface area structure of the nanosheets increases the reaction contact area of Pt. In addition to the changes in the structure of the reactants, the mechanism of the free radical chain reaction [122,123] was also shown to be correct. In short, some researchers agree that Pt acts as an intermediate reactant (electron acceptor transition carrier) in the catalytic process [126,127] to promote the activation of H<sub>2</sub>O<sub>2</sub> into hydroxyl radicals, and then, hydroxyl radicals and TMB undergo redox reactions on the surface of the nanosheets (Figure 9B).

Similarly, scientists found that if and only when the concentration of NP was appropriate, free radicals could promote enzyme activity. Vinita et al. [128] studied Au@MoS<sub>2</sub>-QD NPs and noted that NPs act as electron acceptor transition carriers, triggering the instantaneous decomposition of H<sub>2</sub>O<sub>2</sub> into hydroxyl radicals and promoting electron transfer between H<sub>2</sub>O<sub>2</sub> and TMB, accelerating the production of blue-green light (Figure 9C). In the same year, Wu et al. [129] published the peroxidase activity mechanism of MoSe<sub>2</sub> nanosheets, which accelerated the acquisition of electrons by H<sub>2</sub>O<sub>2</sub> from TMB and accomplished the catalytic oxidation of TMB (Figure 9D). Interestingly, the process of accelerating electron transfer was caused by hydroxyl radicals, but the nanosheets consumed hydroxyl radicals and simultaneously acted as electron transfer media carriers. Perhaps we can



speculate that a certain concentration of nanosheets can more noticeably promote the generation of hydroxyl radicals and accelerate the electron transfer of TMB.

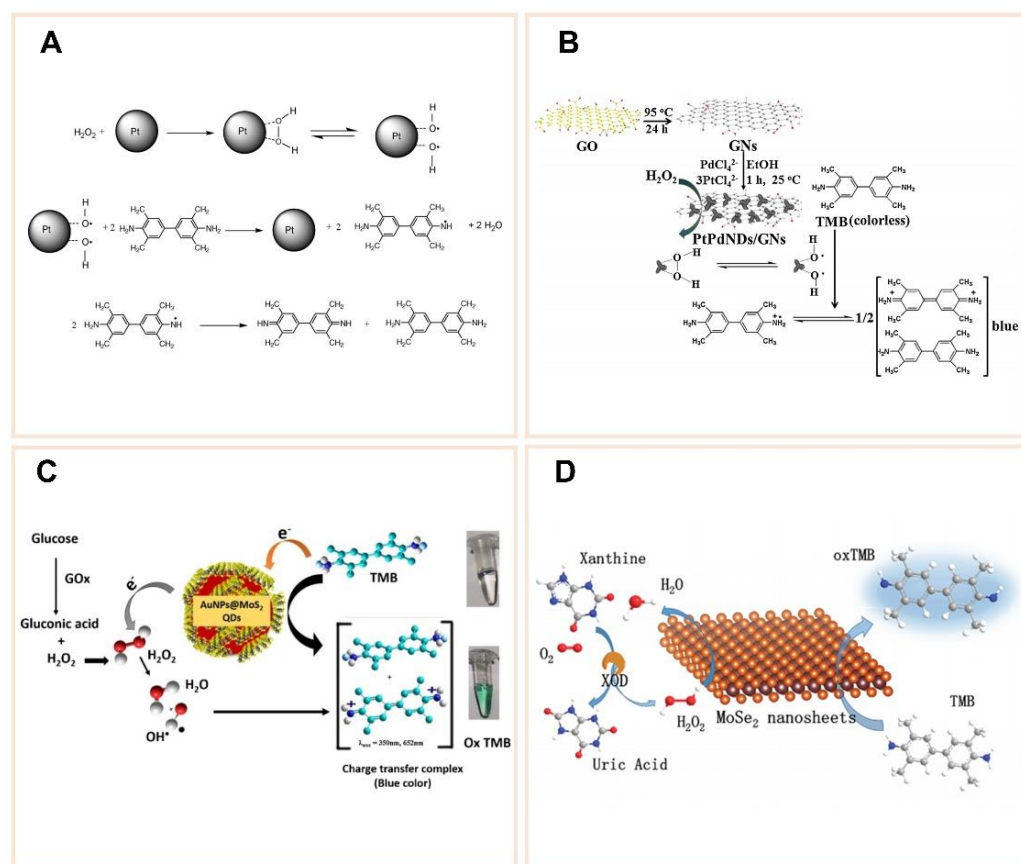


**Figure 9.** Nanozymes modulate energy conversion events by catalyzing the production of free radicals from the interface components: (A) Pt nanozyme, reprinted with permission from reference [124]. Copyright 2011, Elsevier. (B) PtPd nanozyme on GNs (graphene nanosheets), reprinted with permission from reference [125]. Copyright 2014, Elsevier. (C) Au@MoS<sub>2</sub>-QDs (quantum dots) nanozyme, reprinted with permission from reference [128]. Copyright 2018, Elsevier. (D) MoSe<sub>2</sub> nanozyme, all of which promoted enzyme activity by generating highly active hydroxyl radicals, which were converted into light signals. Reprinted with permission from reference [129]. Copyright 2018, Royal Society of Chemistry.

These studies showed that some NPs' biochemical reactions produced hydroxyl free radicals. Therefore, scientists cannot help but predict that enzymes' biochemical events based on the modulation of biological macromolecules are not an exception. For example, Wang et al. [93] once speculated that in the reaction system of nucleic acids, nanozymes, and substrates Fe<sub>3</sub>O<sub>4</sub> NPs and H<sub>2</sub>O<sub>2</sub> coexisted to produce highly reactive hydroxyl radicals (Fenton Chemical), which can degrade nucleic acids. In fact, the experimental results showed that the nucleic acid was not cleaved. This speculation seems unsupported.

In fact, are there any hydroxyl radicals in the interface reaction between nucleic acids and NPs to modulate enzyme activity? Wang et al. [28] speculated that with the help of nucleic acids, g-C<sub>3</sub>N<sub>4</sub> nanosheets acted on H<sub>2</sub>O<sub>2</sub> to generate hydroxyl radicals to promote enzyme activity. Experiments have shown that functional nanosheets can indeed catalyze the production of intermediate hydroxyl radicals, but this was not the reason for the enhanced enzyme activity of nanomaterials. Zhao et al. [121] also predicted that the interface component nucleic acid should be added to assist nanosheet MoS<sub>2</sub>, catalyze the decomposition of H<sub>2</sub>O<sub>2</sub> to generate hydroxyl radicals, and promote electron transfer between TMB and H<sub>2</sub>O<sub>2</sub> at the interface. Unfortunately, it was confirmed that it was not

the generation of highly active free radicals but the role of nanosheets that accelerated electron transfer.

Based on these reports, we preliminarily believe that in the interfacial reaction of nucleic acids and reversible modulation of nanozymes, hydroxyl radicals, which are highly active substances, have not yet been proven. However, in the catalytic reaction of NPs, hydroxyl radicals do exist. Therefore, whether nucleic acids act on nanozymes to inhibit the formation of hydroxyl radicals or whether nucleic acids replace some of the functions of hydroxyl radicals is worthy of further exploration.

#### 4. Conclusions and Outlook

In this article, we focus on the study of nucleic acids as a new interface component that participates in the interface effect of nanozyme biochemical energy conversion events.

Nucleic acids increase the interface free energy of NPs; that is, accompanied by new interface effects, such as the valence state of ions at the interface, the transfer of electron motion and other structure-related properties have undergone considerable changes and therefore have changed the chemical properties of NPs (enzyme activity).

First, the controllable dissociation of nucleic acids confers the reversibility and specificity of nanozyme activity. In addition, the controllable adsorption of nucleic acids by nanozymes converts nucleic acid-specific recognition events into analytical events that can amplify detectable signals, increasing the sensitivity of biochemical energy conversion events. Therefore, in the field of nutrition and safety, there have been an increasing number of studies on functional nanozymes. We analyzed representative examples of the energy conversion of three types of functional nanozymes.

Although many achievements have been made, the modulation of nanozymes is still in the preliminary stage, and there are still many technical roadblocks to practical applications that need to be overcome. Here, a brief summary of the current challenges:

- (1) It should be admitted that there are conflicting conclusions about nucleic acid-modulated nanozymes in the current reported research. Perhaps there were differences in the morphology and composition of nanozymes in different studies or there are other reasons for the differences, so in-depth research is needed.
- (2) Self-assembled nanozymes require a relatively long assembly time, irreversible binding nanozymes have a relatively high cost, and reversible binding nanozymes require further study of the mechanism of their effective modulation. These three points are the focus of future research.
- (3) At present, most functional nanozymes require solution systems for reactions. Therefore, it is still a huge challenge to extend the reaction to solid-phase systems (such as paper-based systems) and to construct cheap, portable integrated devices without sacrificing the activity of the interface components.
- (4) Nanozymes have high catalytic activity and excellent biocompatibility. Nanozymes have been used as antibacterial agents to promote wound healing [130,131]; to assist in tumor cell therapy (such as magnetic hyperthermia, chemodynamic therapy, photothermal therapy, and photodynamic therapy [132–136]); and to alleviate the symptoms of metabolic diseases (such as glucose metabolism: diabetes [45], immune metabolism: inflammation and cancer [137,138]). Most of the nanozymes reported are metal oxides (such as iron oxide, manganese oxide, copper oxide, cerium oxide, etc.) or noble metals (silver, gold, platinum, palladium, cobalt, etc.). They can be degraded and metabolized in the body, and the released metal ions are cytotoxic. Therefore, it is necessary to study the modulation mechanism of biomacromolecules with nanozymes to solve the biocompatibility, targeting, and safety issues of nanozymes in the biomedical field.

**Author Contributions:** X.W. (Xin Wang) formulated the aims, wrote and revised the manuscript. Y.X. researched and summarized the literature. N.C. designed the ideas, wrote and revised the manuscript. X.W. (Xinxian Wang) researched and summarized the literature. K.H. formulated the

aims, discussed the ideas. Y.L. designed the ideas, got the financial support for the project leading to this publication. All authors have read and agreed to the published version of the manuscript.

**Funding:** This research was funded by Natural Science Foundation of China (Grant No. 32001787).

**Acknowledgments:** Nan Cheng would like to thank the the 2115 Talent Development Program of China Agricultural University. Yunbo Luo would like to thank the Shandong Provincial Key Research and Development Program (2019JZZY011014).

**Conflicts of Interest:** The authors declare that they have no competing interests.

## References

1. Zeng, Z.; Zhang, C.; Li, J.; Cui, D.; Jiang, Y.; Pu, K. Activatable Polymer Nanoenzymes for Photodynamic Immunometabolic Cancer Therapy. *Adv. Mater.* **2021**, *33*, e2007247. [[CrossRef](#)]
2. Singh, N.; Naveenkumar, S.K.; Geethika, M.; Mughsh, G. A Cerium Vanadate Nanozyme with Specific Superoxide Dismutase Activity Regulates Mitochondrial Function and ATP Synthesis in Neuronal Cells. *Angew. Chem.* **2020**, *60*, 3121–3130. [[CrossRef](#)]
3. Wei, H.; Wang, E. Nanomaterials with enzyme-like characteristics (nanozymes): Next-generation artificial enzymes. *Chem. Soc. Rev.* **2013**, *42*, 6060–6093. [[CrossRef](#)]
4. Wang, X.; Hu, Y.; Wei, H. Nanozymes in bionanotechnology: From sensing to therapeutics and beyond. *Inorg. Chem. Front.* **2016**, *3*, 41–60. [[CrossRef](#)]
5. Xiong, X.; Huang, Y.; Lin, C.; Liu, X.Y.; Lin, Y. Recent advances in nanoparticulate biomimetic catalysts for combating bacteria and biofilms. *Nanoscale* **2019**, *11*, 22206–22215. [[CrossRef](#)] [[PubMed](#)]
6. Wu, J.; Wang, X.; Wang, Q.; Lou, Z.; Li, S.; Zhu, Y.; Qin, L.; Wei, H. Nanomaterials with enzyme-like characteristics (nanozymes): Next-generation artificial enzymes (II). *Chem. Soc. Rev.* **2018**, *42*, 1004–1067. [[CrossRef](#)] [[PubMed](#)]
7. Breslow, R. Biomimetic Chemistry and Artificial Enzymes: Catalysis by Design. *Acc. Chem. Res.* **1995**, *28*, 146–153. [[CrossRef](#)]
8. Breslow, R.; Overman, L.E. "Artificial enzyme" combining a metal catalytic group and a hydrophobic binding cavity. *J. Am. Chem. Soc.* **1970**, *92*, 1075–1077. [[CrossRef](#)]
9. Huang, Y.; Ren, J.; Qu, X. Nanozymes: Classification, Catalytic Mechanisms, Activity Regulation, and Applications. *Chem. Rev.* **2019**, *119*, 4357–4412. [[CrossRef](#)]
10. Dutta, A.K.; Das, S.; Samanta, P.K.; Roy, S.; Adhikary, B.; Biswas, P. Non-enzymatic amperometric sensing of hydrogen peroxide at a CuS modified electrode for the determination of urine H<sub>2</sub>O<sub>2</sub>. *Electrochim. Acta* **2014**, *144*, 282–287. [[CrossRef](#)]
11. Manea, F.; Houillon, F.B.; Pasquato, L.; Scrimin, P. Nanozymes: Gold-Nanoparticle-Based Transphosphorylation Catalysts. *Angew. Chem. Int. Ed.* **2004**, *116*, 6291–6295. [[CrossRef](#)]
12. Zhou, Y.; Liu, B.; Yang, R.; Liu, J. Filling in the Gaps between Nanozymes and Enzymes: Challenges and Opportunities. *Bioconjug. Chem.* **2017**, *28*, 2903–2909. [[CrossRef](#)] [[PubMed](#)]
13. Cheng, H.; Liu, Y.; Hu, Y.; Ding, Y.; Lin, S.; Cao, W.; Wang, Q.; Wu, J.; Muhammad, F.; Zhao, X. Monitoring of Heparin Activity in Live Rats Using Metal-Organic Framework Nanosheets as Peroxidase Mimics. *Anal. Chem.* **2017**, *89*, 11552–11559. [[CrossRef](#)] [[PubMed](#)]
14. Gao, L.; Zhuang, J.; Nie, L.; Zhang, J.; Zhang, Y.; Gu, N.; Wang, T.; Feng, J.; Yang, D.; Perrett, S. Intrinsic peroxidase-like activity of ferromagnetic nanoparticles. *Nat. Nanotechnol.* **2007**, *2*, 577–583. [[CrossRef](#)]
15. Jiang, B.; Duan, D.; Gao, L.; Zhou, M.; Fan, K.; Tang, Y.; Xi, J.; Bi, Y.; Tong, Z.; Gao, G.F.; et al. Standardized assays for determining the catalytic activity and kinetics of peroxidase-like nanozymes. *Nat. Protoc.* **2018**, *13*, 1506–1520. [[CrossRef](#)] [[PubMed](#)]
16. Lin, Y.; Ren, J.; Qu, X. Catalytically Active Nanomaterials: A Promising Candidate for Artificial Enzymes. *Acc. Chem. Res.* **2014**, *47*, 1097–1105. [[CrossRef](#)]
17. Zhu, X.; Tang, L.; Wang, J.; Peng, B.; Ouyang, X.; Tan, J.; Yu, J.; Feng, H.; Tang, J. Enhanced peroxidase-like activity of boron nitride quantum dots anchored porous CeO<sub>2</sub> nanorods by aptamer for highly sensitive colorimetric detection of kanamycin. *Sens. Actuators B Chem.* **2020**, *330*, 129318. [[CrossRef](#)]
18. Aiba, Y.; Sumaoka, J.; Komiyama, M. Artificial DNA cutters for DNA manipulation and genome engineering. *Chem. Soc. Rev.* **2011**, *40*, 5657–5668. [[CrossRef](#)]
19. Maruthupandy, M.; Rajivgandhi, G.; Muneeswaran, T.; Vennila, T.; Quero, F.; Song, J.M. Chitosan/silver nanocomposites for colorimetric detection of glucose molecules—ScienceDirect. *Int. J. Biol. Macromol.* **2019**, *121*, 822–828. [[CrossRef](#)] [[PubMed](#)]
20. Gooding, J.J. Big Moves in Biosensing. *ACS Sens.* **2016**, *1*, 633. [[CrossRef](#)]
21. Gooding, J.J. The Exciting World of Single Molecule Sensors. *ACS Sens.* **2016**, *1*, 1163–1164. [[CrossRef](#)]
22. Gooding, J.J.; Gaus, K. Single-Molecule Sensors: Challenges and Opportunities for Quantitative Analysis. *Angew. Chem. Int. Ed.* **2016**, *55*, 11354–11366. [[CrossRef](#)] [[PubMed](#)]
23. Wu, J.; Li, S.; Wei, H. Integrated nanozymes: Facile preparation and biomedical applications. *Chem. Commun.* **2018**, *54*, 6520–6530. [[CrossRef](#)]
24. Liang, M.; Yan, X. Nanozymes: From New Concepts, Mechanisms, and Standards to Applications. *Acc. Chem. Res.* **2019**, *52*, 2190–2200. [[CrossRef](#)]

25. Guo, L.; Huang, K.; Liu, H. Biocompatibility selenium nanoparticles with an intrinsic oxidase-like activity. *J. Nanoparticle Res.* **2016**, *18*, 1–10. [[CrossRef](#)]
26. Pu, F.; Ren, J.; Qu, X. Nucleobases, nucleosides, and nucleotides: Versatile biomolecules for generating functional nanomaterials. *Chem. Soc. Rev.* **2018**, *47*, 11285–11306.
27. Zhang, X.; Liu, Y.; Gopalakrishnan, S.; Castellanos-Garcia, L.; Li, G.; Malassine, M.; Uddin, I.; Huang, R.; Luther, D.C.; Vachet, R.W.; et al. Intracellular Activation of Bioorthogonal Nanozymes through Endosomal Proteolysis of the Protein Corona. *ACS Nano* **2020**, *14*, 4767–4773. [[CrossRef](#)]
28. Wang, Y.M.; Liu, J.W.; Adkins, G.B.; Shen, W.; Trinh, M.P.; Duan, L.Y.; Jiang, J.H.; Zhong, W. Enhancement of the Intrinsic Peroxidase-Like Activity of Graphitic Carbon Nitride Nanosheets by ssDNAs and Its Application for Detection of Exosomes. *Anal. Chem.* **2017**, *89*, 12327–12333. [[CrossRef](#)]
29. Li, X.; Zhao, Y. Synthetic glycosidases for the precise hydrolysis of oligosaccharides and polysaccharides. *Chem. Sci.* **2021**, *12*, 374–383. [[CrossRef](#)]
30. Zhang, D.; Zhao, Y.X.; Gao, Y.J.; Gao, F.P.; Fan, Y.S.; Li, X.J.; Duan, Z.Y.; Wang, H. Anti-bacterial and in vivo tumor treatment by reactive oxygen species generated by magnetic nanoparticles. *J. Mater. Chem. B* **2013**, *1*, 5100–5107. [[CrossRef](#)]
31. Ma, J.; Qiu, J.; Wang, S. Nanozymes for Catalytic Cancer Immunotherapy. *ACS Appl. Nano Mater.* **2020**, *3*, 4925–4943. [[CrossRef](#)]
32. Taoli, D.; Jing, Y.; Victor, P.; Nan, Z.; Zuhong, L.; Yonggang, K.; Cheng, Z. DNA nanotechnology assisted nanopore-based analysis. *Nucleic Acids Res.* **2020**, *48*, 2791–2806.
33. Sivakova, S.; Rowan, S.J. Nucleobases as Supramolecular Motifs. *Chem. Form.* **2005**, *34*, 9–21.
34. Zhou, P.; Shi, R.; Yao, J.F.; Sheng, C.F.; Li, H. Supramolecular self-assembly of nucleotide–metal coordination complexes: From simple molecules to nanomaterials. *Coord. Chem. Rev.* **2016**, *46*, 107–143.
35. Verma, S.; Mishra, A.K.; Kumar, J. The Many Facets of Adenine: Coordination, Crystal Patterns, and Catalysis. *Acc. Chem. Res.* **2010**, *43*, 79–91. [[CrossRef](#)] [[PubMed](#)]
36. Ciesielski, A.; Garah, M.E.; Masiero, S.; Samorì, P. Self-assembly of Natural and Unnatural Nucleobases at Surfaces and Interfaces. *Small* **2015**, *12*, 83–95. [[CrossRef](#)] [[PubMed](#)]
37. Peters, G.M.; Davis, J.T. Supramolecular Gels Made from Nucleobase, Nucleoside and Nucleotide Analogs. *Chem. Soc. Rev.* **2016**, *45*, 3188–3206. [[CrossRef](#)]
38. CRC Press. *DNA Nanotechnology*; CRC Press: Boca Raton, FL, USA, 2014.
39. Lu, C.H.; Ceconello, A.; Willner, I. Recent Advances in the Synthesis and Functions of Reconfigurable Interlocked DNA Nanostructures. *J. Am. Chem. Soc.* **2016**, *138*, 5172–5185. [[CrossRef](#)]
40. Aoki, K.; Murayama, K. Nucleic Acid-Metal Ion Interactions in the Solid State. In *Interplay between Metal Ions and Nucleic Acids*; Sigel, A., Sigel, H., Sigel, R.K., Eds.; Springer Science Business Media: Berlin, Germany, 2012; Volume 10, pp. 43–102. [[CrossRef](#)]
41. Sigel, H.; Griesser, R. Nucleoside 5'-triphosphates: Self-association, Acid–base, and Metal Ion-binding properties in Solution. *Chem. Soc. Rev.* **2005**, *34*, 875–900. [[CrossRef](#)]
42. Shen, X.; Liu, W.; Gao, X.; Lu, Z.; Wu, X.; Gao, X. Mechanisms of Oxidase and Superoxide Dismutation-like Activities of Gold, Silver, Platinum, and Palladium, and Their Alloys: A General Way to the Activation of Molecular Oxygen. *J. Am. Chem. Soc.* **2015**, *137*, 15882–15891. [[CrossRef](#)]
43. Weerathunge, P.; Ramanathan, R.; Torok, V.A.; Hodgson, K.; Xu, Y.; Goodacre, R.; Behera, B.K.; Bansal, V. Ultrasensitive Colorimetric Detection of Murine Norovirus Using NanoZyme Aptasensor. *Anal. Chem.* **2019**, *91*, 3270–3276. [[CrossRef](#)] [[PubMed](#)]
44. Zhan, L.; Li, C.M.; Wu, W.B.; Huang, C.Z. A Colorimetric Immunoassay for Respiratory Syncytial Virus Detection Based on gold Nanoparticles–Graphene Oxide Hybrids with Mercury-Enhanced Peroxidase-like Activity. *Chem. Commun.* **2014**, *50*, 11526–11528. [[CrossRef](#)] [[PubMed](#)]
45. Zhou, Y.; Liu, C.; Yu, Y.; Yin, M.; Sun, J.; Huang, J.; Chen, N.; Wang, H.; Fan, C.; Song, H. An Organelle-Specific Nanozyme for Diabetes Care in Genetically or Diet-Induced Models. *Adv. Mater.* **2020**, *32*, 2003708. [[CrossRef](#)]
46. Gao, P.; Chang, X.; Zhang, D.; Cai, Y.; Chen, G.; Wang, H.; Wang, T.; Kong, T. Synergistic Integration of Metal Nanoclusters and Biomolecules as Hybrid Systems for Therapeutic Applications. *Acta Pharm. Sin. B* **2020**. [[CrossRef](#)]
47. Wei, M.; Qiao, Y.; Zhao, H.; Liang, J.; Li, T.S.; Luo, Y.; Lu, S.; Shi, X.; Lu, W.; Sun, X. Electrochemical Non-enzymatic Glucose Sensors: Recent Progress and Perspectives. *Chem. Commun.* **2020**, *56*, 14553–14569. [[CrossRef](#)]
48. Lo, N.; Hsu, W.; Chen, Y.; Sun, I.; Chen, P. Facile Nonenzymatic Glucose Electrode Composed of Commercial CuO Powder and Ionic Liquid Binder. *Electroanalysis* **2020**. [[CrossRef](#)]
49. Qian, X.; Westensee, I.N.; Brodzkij, E.; Städler, B. Cell mimicry as a Bottom-up Strategy for Hierarchical Engineering of Nature-inspired Entities. *Wiley Interdiscip. Rev. Nanomed. Nanobiotechnol.* **2021**, *13*, e1683. [[CrossRef](#)] [[PubMed](#)]
50. Goswami, N.; Zheng, K.; Xie, J. Bio-NCs—the marriage of ultrasmall metal nanoclusters with biomolecules. *Nanoscale* **2014**, *6*, 13328–13347. [[CrossRef](#)]
51. Tao, X.; Wang, X.; Liu, B.; Liu, J. Conjugation of antibodies and aptamers on nanozymes for developing biosensors. *Biosens. Bioelectron.* **2020**, *168*, 112537. [[CrossRef](#)]
52. Shang, L.; Dong, S.; Nienhaus, G.U. Ultra-small fluorescent metal nanoclusters: Synthesis and biological applications. *Nano Today* **2011**, *6*, 401–418. [[CrossRef](#)]

53. Tanaka, S.I.; Miyazaki, J.; Tiwari, D.K.; Jin, T.; Inouye, Y. Fluorescent Platinum Nanoclusters: Synthesis, Purification, Characterization, and Application to Bioimaging. *Angew. Chem. Int. Ed.* **2011**, *123*, 451–455. [[CrossRef](#)]
54. Kawasaki, H.; Yamamoto, H.; Fujimori, H.; Arakawa, R.; Inada, M.; Iwasaki, Y. Surfactant-free solution synthesis of fluorescent platinum subnanoclusters. *Chem. Commun.* **2010**, *46*, 3759–3761. [[CrossRef](#)]
55. Dahm, R. Friedrich Miescher and the discovery of DNA. *Dev. Biol.* **2005**, *278*, 274–288. [[CrossRef](#)] [[PubMed](#)]
56. Fu, Y.; Zhao, X.; Zhang, J.; Li, W. DNA-Based Platinum Nanozymes for Peroxidase Mimetics. *J. Phys. Chem. C* **2014**, *118*, 18116–18125. [[CrossRef](#)]
57. Sun, Y.; Wang, J.; Li, W.; Zhang, J.; Zhang, Y.; Fu, Y. DNA-stabilized bimetallic nanozyme and Its application on colorimetric assay of biothiols. *Biosens. Bioelectron.* **2015**, *74*, 1038–1046. [[CrossRef](#)]
58. Chen, W.; Fang, X.; Li, H.; Cao, H.; Kong, J. DNA-mediated inhibition of peroxidase-like activities on platinum nanoparticles for simple and rapid colorimetric detection of nucleic acids. *Biosens. Bioelectron.* **2017**, *94*, 169. [[CrossRef](#)]
59. Chen, W.; Fang, X.; Ye, X.; Wang, X.; Kong, J. Colorimetric DNA assay by exploiting the DNA-controlled peroxidase mimicking activity of mesoporous silica loaded with platinum nanoparticles. *Microchim. Acta* **2018**, *185*, 544. [[CrossRef](#)]
60. Higuchi, A.; Siao, Y.D.; Yang, S.T.; Hsieh, P.V.; Fukushima, H.; Chang, Y.; Ruan, R.C.; Chen, W.Y. Preparation of a DNA aptamer-Pt complex and its use in the colorimetric sensing of thrombin and anti-thrombin antibodies. *Anal. Chem.* **2008**, *80*, 6580–6586. [[CrossRef](#)] [[PubMed](#)]
61. Kumar, C.V.; Asuncion, E.H. DNA binding studies and site selective fluorescence sensitization of an anthryl probe. *J. Am. Chem. Soc.* **1993**, *115*, 8547–8553. [[CrossRef](#)]
62. Moradi, S.Z.; Nowroozi, A.; Sadrjavadi, K.; Moradi, S.; Mansouri, K.; Hosseinzadeh, L.; Shahlaei, M. Direct evidences for the groove binding of the Clomifene to double stranded DNA. *Int. J. Biol. Macromol.* **2018**, *114*, 40–53. [[CrossRef](#)]
63. Hu, P.; Han, L.; Zhu, C.; Dong, S.J. Nanoreactors: A novel biosensing platform for protein assay. *Chem. Commun.* **2013**, *49*, 1705–1707. [[CrossRef](#)]
64. Zhang, L.; Qi, Z.; Zou, Y.; Zhang, J.; Tang, Z. Engineering DNA-Nanozyme Interfaces for Rapid Detection of Dental Bacteria. *ACS Appl. Mater. Interfaces* **2019**, *11*, 30640–30647. [[CrossRef](#)]
65. Zhang, L.; Huang, R.; Liu, W.; Liu, H.; Zhou, X.; Xing, D. Rapid and visual detection of *Listeria monocytogenes* based on nanoparticle cluster catalyzed signal amplification. *Biosens. Bioelectron.* **2016**, *86*, 1–7. [[CrossRef](#)]
66. Zhang, Z.; Wang, Z.; Wang, X.; Yang, X. Magnetic nanoparticle-linked colorimetric aptasensor for the detection of thrombin. *Sens. Actuators B Chem.* **2010**, *147*, 428–433.
67. Sun, D.; Lin, X.; Lu, J.; Wei, P.; Zhang, L. DNA nanotetrahedron-assisted electrochemical aptasensor for cardiac troponin I detection based on the co-catalysis of hybrid nanozyme, natural enzyme and artificial DNAzyme. *Biosens. Bioelectron.* **2019**, *142*, 111578. [[CrossRef](#)]
68. Dehghani, Z.; Nguyen, T.; Golabi, M.; Hosseini, M.; Rezayan, A.H.; Mohammadnejad, J.; Wolff, A.; Vinayaka, A.C. Magnetic beads modified with Pt/Pd nanoparticle and aptamer as a catalytic nano-bioprobe in combination with loop mediated isothermal amplification for the on-site detection of *Salmonella Typhimurium* in food and fecal samples. *Food Control.* **2021**, *121*, 107664. [[CrossRef](#)]
69. Wu, Y.; Li, G.; Zou, L.; Lei, S.; Yu, Q.; Ye, B. Highly active DNAzyme-peptide hybrid structure coupled porous palladium for high-performance electrochemical aptasensing platform. *Sens. Actuators* **2018**, *259*, 372–379. [[CrossRef](#)]
70. An, J.; Li, G.; Zhang, Y.; Zhang, T.; Fan, H. Recent Advances in Enzyme-Nanostructure Biocatalysts with Enhanced Activity. *Catalysts* **2020**, *10*, 338. [[CrossRef](#)]
71. Liu, B.; Liu, J. Surface modification of nanozymes. *Nano Res.* **2017**, *10*, 1125–1148. [[CrossRef](#)]
72. Zhao, Y.; Dai, X.; Wang, F.; Zhang, X.; Fan, C.; Liu, X. Nanofabrication based on DNA nanotechnology. *Nano Today* **2019**, *26*, 123–148. [[CrossRef](#)]
73. Ito, Y.; Hasuda, H. Immobilization of DNAzyme as a thermostable biocatalyst. *Biotechnol. Bioeng.* **2010**, *86*, 72–77. [[CrossRef](#)]
74. Santos, F.D.J.N.D.; Ximenes, V.F.; da Fonseca, L.M.; Oliveira, O.M.M.D.F.; Brunetti, I.L. Horseradish Peroxidase-Catalyzed Oxidation of Rifampicin: Reaction Rate Enhancement by Co-oxidation with Anti-inflammatory Drugs. *Biol. Pharm. Bull.* **2005**, *28*, 1822–1826. [[CrossRef](#)] [[PubMed](#)]
75. Sentchouk, V.V.; Grintsevich, E.E. Oxidation of benzidine and its derivatives by thyroid peroxidase. *Biochem. Biokhimiia* **2004**, *69*, 201. [[CrossRef](#)] [[PubMed](#)]
76. Fan, J.; Yin, J.-J.; Ning, B.; Wu, X.; Hu, Y.; Ferrari, M.; Anderson, G.J.; Wei, J.; Zhao, Y.; Nie, G. Direct evidence for catalase and peroxidase activities of ferritin-platinum nanoparticles. *Biomaterials* **2011**, *32*, 1611–1618. [[CrossRef](#)] [[PubMed](#)]
77. Fan, C.; Pei, H. Special Issue of "DNA Nanotechnology". *Chin. J. Chem.* **2016**. [[CrossRef](#)]
78. Yao, G.; Li, J.; Chao, J.; Pei, H.; Liu, H.; Zhao, Y.; Shi, J.; Huang, Q.; Wang, L.; Huang, W.; et al. Gold-Nanoparticle-Mediated Jigsaw-Puzzle-like Assembly of Supersized Plasmonic DNA Origami. *Angew. Chem.* **2015**. [[CrossRef](#)]
79. Chen, F.; Bai, M.; Cao, K.; Zhao, Y.; Wei, J.; Zhao, Y. Fabricating MnO<sub>2</sub> Nanozymes as Intracellular Catalytic DNA Circuit Generators for Versatile Imaging of Base-Excision Repair in Living Cells. *Adv. Funct. Mater.* **2017**, *27*, 1702748. [[CrossRef](#)]
80. Wang, H.; Yang, R.; Yang, L.; Tan, W. Nucleic Acid Conjugated Nanomaterials for Enhanced Molecular Recognition. *ACS Nano* **2009**, *3*, 2451. [[CrossRef](#)]
81. Liu, J. Adsorption of DNA onto gold nanoparticles and graphene oxide: Surface science and applications. *Phys. Chem. Chem. Phys.* **2012**, *14*, 10485–10496. [[CrossRef](#)]

82. Pautler, R.; Kelly, E.Y.; Huang, P.J.J.; Cao, J.; Liu, B.; Liu, J. Attaching DNA to Nanoceria: Regulating Oxidase Activity and Fluorescence Quenching. *ACS Appl. Mater. Interfaces* **2013**, *5*, 6820–6825. [[CrossRef](#)]
83. Yang, R.; Jin, J.; Chen, Y.; Shao, N.; Tan, W. Carbon Nanotube–Quenched Fluorescent Oligonucleotides: Probes that Fluoresce upon Hybridization. *J. Am. Chem. Soc.* **2008**, *130*, 8351–8358. [[CrossRef](#)]
84. Lu, C.H.; Yang, H.H.; Zhu, C.L.; Chen, X.; Chen, G.N. A Graphene Platform for Sensing Biomolecules & dagger. *Angew. Chem.* **2009**, *48*, 4785–4787.
85. He, S.; Song, B.; Li, D.; Zhu, C.; Qi, W.; Wen, Y.; Wang, L.; Song, S.; Fang, H.; Fan, C. A Graphene Nanoprobe for Rapid, Sensitive, and Multicolor Fluorescent DNA Analysis. *Adv. Funct. Mater.* **2010**, *20*, 453–459. [[CrossRef](#)]
86. Li, H.; Rothberg, L.J. Label-Free Colorimetric Detection of Specific Sequences in PCR amplified DNA. In Proceedings of the 2005 NSTI Nanotechnology Conference and Trade Show (NSTI Nanotech 2005), Anaheim, CA, USA, 8–12 May 2005; Volume 1.
87. Zhang, X.; Liu, B.; Dave, N.; Servos, M.R.; Liu, J. Instantaneous Attachment of an Ultrahigh Density of Nonthiolated DNA to Gold Nanoparticles and Its Applications. *Langmuir ACS J. Surf. Colloids* **2012**, *28*, 17053–17060. [[CrossRef](#)]
88. Pei, H.; Li, F.; Wan, Y.; Wei, M.; Fan, C. Designed Diblock Oligonucleotide for the Synthesis of Spatially Isolated and Highly Hybridizable Functionalization of DNA–Gold Nanoparticle Nanoconjugates. *J. Am. Chem. Soc.* **2012**, *134*, 11876–11879. [[CrossRef](#)]
89. Saha, K.; Agasti, S.S.; Kim, C.; Li, X.; Rotello, V.M. Gold Nanoparticles in Chemical and Biological Sensing. *Chem. Rev.* **2012**, *112*, 2739–2779. [[CrossRef](#)] [[PubMed](#)]
90. Li, X.; Song, J.; Chen, B.L.; Wang, B.; Li, R.; Jiang, H.M.; Liu, J.F.; Li, C.Z. A label-free colorimetric assay for detection of c-Myc mRNA based on peptide nucleic acid and silver nanoparticles. *Sci. Bull.* **2016**, *61*, 1–6. [[CrossRef](#)]
91. Bülbül, G.; Hayat, A.; Andreescu, S. ssDNA-Functionalized Nanoceria: A Redox-Active Aptaswitch for Biomolecular Recognition. *Adv. Heal. Mater.* **2016**, *5*, 822–828. [[CrossRef](#)] [[PubMed](#)]
92. Zhao, W.; Chiuman, W.; Lam, J.C.; McManus, S.A.; Chen, W.; Cui, Y.; Pelton, R.; Brook, M.A.; Li, Y. DNA Aptamer Folding on Gold Nanoparticles: From Colloid Chemistry to Biosensors. *J. Am. Chem. Soc.* **2008**, *130*, 3610–3618. [[CrossRef](#)]
93. Wang, L.; Huang, Z.; Liu, Y.; Wu, J.; Liu, J. Fluorescent DNA Probing Nanoscale MnO<sub>2</sub>: Adsorption, Dissolution by Thiol, and Nanozyme Activity. *Langmuir* **2018**, *34*, 3094–3101. [[CrossRef](#)]
94. Liu, B.; Liu, J. Accelerating peroxidase mimicking nanozymes using DNA. *Nanoscale* **2015**, *7*, 13831–13835. [[CrossRef](#)]
95. Li, S.; Zhao, X.; Yu, X.; Wan, Y.; Wang, H. Fe<sub>3</sub>O<sub>4</sub> Nanozymes with Aptamer-Tuned Catalysis for Selective Colorimetric Analysis of ATP in Blood. *Anal. Chem.* **2019**, *91*, 14737–14742. [[CrossRef](#)]
96. Huo, Y.; Qi, L.; Lv, X.J.; Lai, T.; Zhang, J.; Zhang, Z.Q. A sensitive aptasensor for colorimetric detection of adenosine triphosphate based on the protective effect of ATP-aptamer complexes on unmodified gold nanoparticles. *Biosens. Bioelectron.* **2016**, *78*, 315–320. [[CrossRef](#)]
97. Zhang, C.; Rissman, R.A.; Feng, J. Characterization of ATP Alternations in an Alzheimer’s Transgenic Mouse Model. *J. Alzheimer Dis.* **2015**, *44*, 375–378. [[CrossRef](#)] [[PubMed](#)]
98. Deng, J.; Wang, K.; Wang, M.; Yu, P.; Mao, L. Mitochondria Targeted Nanoscale Zeolitic Imidazole Framework-90 (ZIF-90) for ATP Imaging in Live Cells. *J. Am. Chem. Soc.* **2017**, *139*, 5877–5882. [[CrossRef](#)]
99. Woong, J.Y.; Wang, T.; Sekyu, H.; Dokyoung, K.; Ma, D.; Hean, K.K.; Sungjee, K.; Junyang, J.; Han, A.K. A Ratiometric Two-Photon Fluorescent Probe for Tracking the Lysosomal ATP Level: Direct in cellulo Observation of Lysosomal Membrane Fusion Processes. *Angew. Chem. Int. Ed.* **2018**, *130*, 10299–10304.
100. Kim, J.H.; Ahn, J.H.; Barone, P.W.; Jin, H.; Strano, M.S. A Luciferase/Single-Walled Carbon Nanotube Conjugate for Near-Infrared Fluorescent Detection of Cellular ATP. *Angew. Chem. Int. Ed.* **2010**, *49*, 1456–1459. [[CrossRef](#)]
101. Lindsay, V.N.G.; Viart, H.M.-F.; Sarpong, R.; And, H.M.-F.V. ChemInform Abstract: Stereodivergent Intramolecular C(sp<sup>3</sup>)-H Functionalization of Azavinyl Carbenes: Synthesis of Saturated Heterocycles and Fused N-Heterocycles. *ChemInform* **2015**, *46*, 8368. [[CrossRef](#)]
102. Kashefi-Kheyraadi, L.; Mehrgardi, M.A. Aptamer-conjugated silver nanoparticles for electrochemical detection of adenosine triphosphate. *Biosens. Bioelectron.* **2012**, *37*, 94–98. [[CrossRef](#)]
103. Wang, J.; Wang, L.; Liu, X.; Liang, Z.; Song, S.; Li, W.; Li, G.; Fan, C. A Gold Nanoparticle-Based Aptamer Target Binding Readout for ATP Assay. *Adv. Mater.* **2007**, *19*, 3943–3946. [[CrossRef](#)]
104. Hizir, M.S.; Top, M.; Balcioglu, M.; Rana, M.; Robertson, N.M.; Shen, F.; Sheng, J.; Yigit, M.V. Multiplexed Activity of perAoxidase: DNA-Capped AuNPs Act as Adjustable Peroxidase. *Anal. Chem.* **2016**, *88*, 600–605. [[CrossRef](#)]
105. Li, Z.-M.; Zhong, X.-L.; Wen, S.-H.; Zhang, L.; Liang, R.-P.; Qiu, J.-D. Colorimetric detection of methyltransferase activity based on the enhancement of CoOOH nanozyme activity by ssDNA. *Sens. Actuators B Chem.* **2019**, *281*, 1073–1079. [[CrossRef](#)]
106. Liu, B.; Huang, Z.; Liu, J. Boosting the oxidase mimicking activity of nanoceria by fluoride capping: Rivaling protein enzymes and ultrasensitive F<sup>−</sup>-detection. *Nanoscale* **2016**, *8*, 13562–13567. [[CrossRef](#)] [[PubMed](#)]
107. Yang, D.; Fa, M.; Gao, L.; Zhao, R.; Luo, Y.; Yao, X. The Effect of DNA on the Oxidase Activity of Nanoceria with Different Morphologies. *Nanotechnology* **2018**, *29*, 385101. [[CrossRef](#)]
108. Zhang, Y.; Zhou, K.; Zhai, Y.; Qin, F.; Pan, L.; Yao, X. Crystal plane effects of nano-CeO<sub>2</sub> on its antioxidant activity. *Rsc Adv.* **2014**, *4*, 50325–50330. [[CrossRef](#)]
109. Heckert, E.G.; Karakoti, A.S.; Seal, S.; Self, W.T. The role of cerium redox state in the SOD mimetic activity of nanoceria. *Biomaterials* **2008**, *29*, 2705–2709. [[CrossRef](#)] [[PubMed](#)]

110. Pirmohamed, T.; Dowding, J.M.; Singh, S.; Wasserman, B.; Heckert, E.; Karakoti, A.S.; King, J.E.S.; Seal, S.; Self, W.T. Nanoceria exhibit redox state-dependent catalase mimetic activity. *Chem. Commun.* **2010**, *46*, 2736–2738. [[CrossRef](#)] [[PubMed](#)]
111. Ge, C.; Fang, G.; Shen, X.; Chong, Y.; Wamer, W.G.; Gao, X.; Chai, Z.; Chen, C.; Yin, J.J. Facet Energy versus Enzyme-like Activities: The Unexpected Protection of Palladium Nanocrystals against Oxidative Damage. *ACS Nano* **2016**, *10*, 10436. [[CrossRef](#)] [[PubMed](#)]
112. Peterson, G.W.; Lu, A.X.; Epps, I.; Thomas, H. Tuning the Morphology and Activity of Electrospun Polystyrene/ UiO-66-NH<sub>2</sub> Metal-Organic Framework Composites to Enhance Chemical Warfare Agent Removal. *ACS Appl. Mater. Interfaces* **2017**, *9*, 32248–32254. [[CrossRef](#)]
113. Singh, N.; Geethika, M.; Muges, G.; Motika, G.; Eswarappa, S.M. Manganese-Based Nanozymes: Multienzyme Redox Activity and Effect on the Nitric Oxide Produced by Endothelial Nitric Oxide Synthase. *Chem. A Eur. J.* **2018**, *24*, 8393–8403. [[CrossRef](#)]
114. Fang, G.; Li, W.; Shen, X.; Perez-Aguilar, J.M.; Chong, Y.; Gao, X.; Chai, Z.; Chen, C.; Ge, C.; Zhou, R. Differential Pd-nanocrystal facets demonstrate distinct antibacterial activity against Gram-positive and Gram-negative bacteria. *Nat. Commun.* **2018**, *9*, 1–9. [[CrossRef](#)]
115. Baldim, V.; Bedioui, F.; Mignet, N.; Margail, I.; Berret, J.F. The enzyme-like catalytic activity of cerium oxide nanoparticles and its dependency on Ce<sup>3+</sup> surface area concentration. *Nanoscale* **2018**, *10*, 6971–6980. [[CrossRef](#)]
116. Zhang, W.; Dong, J.; Wu, Y.; Cao, P.; Song, L.; Ma, M.; Gu, N.; Zhang, Y. Shape-dependent enzyme-like activity of Co<sub>3</sub>O<sub>4</sub> nanoparticles and their conjugation with his-tagged EGFR single-domain antibody. *Colloids Surf. B Biointerfaces* **2017**, *154*, 55–62. [[CrossRef](#)]
117. Schaate, A.; Roy, P.; Godt, A.; Lippke, J.; Waltz, F.; Wiebcke, M.; Behrens, P. Modulated Synthesis of Zr-Based Metal–Organic Frameworks: From Nano to Single Crystals. *Chem. A Eur. J.* **2011**, *17*, 6643–6651. [[CrossRef](#)] [[PubMed](#)]
118. Peng, F.F.; Zhang, Y.; Gu, N. Size-dependent peroxidase-like catalytic activity of Fe<sub>3</sub>O<sub>4</sub> nanoparticles. *Chin. Chem. Lett.* **2008**, *19*, 730–733. [[CrossRef](#)]
119. Asati, A.; Santra, S.; Kaittanis, C.; Nath, S.; Perez, J.M. Oxidase-Like Activity of Polymer-Coated Cerium Oxide Nanoparticles. *Angew. Chem.* **2009**, *121*, 2344–2348. [[CrossRef](#)]
120. Huang, L.; Chen, K.; Zhang, W.; Zhu, W.; Liu, X.; Wang, J.; Wang, R.; Hu, N.; Suo, Y.; Wang, J. ssDNA-tailorable oxidase-mimicking activity of spinel MnCo<sub>2</sub>O<sub>4</sub> for sensitive biomolecular detection in food sample. *Sens. Actuators B Chem.* **2018**, *269*, 79–87. [[CrossRef](#)]
121. Zhao, L.; Wang, J.; Su, D.; Zhang, Y.; Lu, H.; Yan, X.; Bai, J.; Gao, Y.; Lu, G. The DNA controllable peroxidase mimetic activity of MoS<sub>2</sub> nanosheets for constructing a robust colorimetric biosensor. *Nanoscale* **2020**, *12*, 12. [[CrossRef](#)] [[PubMed](#)]
122. Kitajima, N.; Fukuzumi, S.; Ono, Y. Formation of superoxide ion during the decomposition of hydrogen peroxide on supported metal oxides. *J. Phys. Chem.* **1978**, *82*, 1505–1509. [[CrossRef](#)]
123. Mochida, I.; Takeshita, K. Transition metal ions on molecular sieves. II. Catalytic activities of transition metal ions on molecular sieves for the decomposition of hydrogen peroxide. *J. Phys. Chem.* **1974**, *78*, 1653–1657. [[CrossRef](#)]
124. Ma, M.; Zhang, Y.; Gu, N. Peroxidase-like catalytic activity of cubic Pt nanocrystals. *Colloids Surf. A Physicochem. Eng. Asp.* **2011**, *373*, 6–10. [[CrossRef](#)]
125. Chen, X.; Su, B.; Cai, Z.; Chen, X.; Oyama, M. PtPd nanodendrites supported on graphene nanosheets: A peroxidase-like catalyst for colorimetric detection of H<sub>2</sub>O<sub>2</sub>. *Sens. Actuators B Chem.* **2014**, *201*, 286–292. [[CrossRef](#)]
126. Aiuchi, T.; Nakajo, S.; Nakaya, K. Reducing Activity of Colloidal Platinum Nanoparticles for Hydrogen Peroxide, 2,2-Diphenyl-1-picrylhydrazyl Radical and 2,6-Dichlorophenol Indophenol. *Biol. Pharm. Bull.* **2004**, *27*, 736–738. [[CrossRef](#)] [[PubMed](#)]
127. Sriphathoorat, R.; Wang, K.; Luo, S.; Tang, M.; Du, H.; Du, X.; Shen, P.K. Well-defined PtNiCo core-shell nanodendrites with enhanced catalytic performance for methanol oxidation. *J. Mater. Chem. A* **2016**, *4*, 18015–18021. [[CrossRef](#)]
128. Vinita, N.N.; Nirala, N.R.; Prakash, R. One step synthesis of AuNPs@MoS<sub>2</sub> -QDs composite as a robust peroxidase- mimetic for instant unaided eye detection of glucose in serum, saliva and tear. *Sens. Actuators B Chem.* **2018**, *263*, 109–119, S0925400518303630. [[CrossRef](#)]
129. Wu, X.; Chen, T.; Wang, J.; Yang, G. Few-layered MoSe<sub>2</sub> nanosheets as an efficient peroxidase nanozyme for highly sensitive colorimetric detection of H<sub>2</sub>O<sub>2</sub> and xanthine. *J. Mater. Chem. B* **2018**, *6*, 105–111. [[CrossRef](#)] [[PubMed](#)]
130. Hu, W.C.; Younis, M.R.; Zhou, Y.; Wang, C.; Xia, X.H. Antibacterial Therapy: In Situ Fabrication of Ultrasmall Gold Nanoparticles/2D MOFs Hybrid as Nanozyme for Antibacterial Therapy. *Small* **2020**, *16*, 2070130. [[CrossRef](#)]
131. Niu, J.; Sun, Y.; Wang, F.; Zhao, C.; Ren, J.; Qu, X. Photo-modulated Nanozyme Used for Gram-Selective Antimicrobial. *Chem. Mater.* **2018**, *30*, 7027–7033. [[CrossRef](#)]
132. Sang, Y.; Cao, F.; Li, W.; Zhang, L.; You, Y.; Deng, Q.; Dong, K.; Ren, J.; Qu, X. Bioinspired Construction of a Nanozyme-Based H<sub>2</sub>O<sub>2</sub> Homeostasis Disruptor for Intensive Chemodynamic Therapy. *J. Am. Chem. Soc.* **2020**, *142*, 5177–5183. [[CrossRef](#)] [[PubMed](#)]
133. Qiu, K.; Wang, J.; Rees, T.W.; Ji, L.; Zhang, Q.; Chao, H. A mitochondria-targeting photothermogenic nanozyme for MRI-guided mild photothermal therapy. *Chem. Commun.* **2018**, *54*, 14108–14111. [[CrossRef](#)]
134. Li, X.; Zhao, C.; Deng, G.; Liu, W.; Shao, J.; Zhou, Z.; Liu, F.; Yang, H.; Yang, S. Nanozyme-Augmented Tumor Catalytic Therapy by Self-Supplied H<sub>2</sub>O<sub>2</sub> Generation. *ACS Appl. Bio Mater.* **2020**, *3*, 1769–1778. [[CrossRef](#)]
135. Chang, M.; Wang, M.; Wang, M.; Shu, M.; Ding, B.; Li, C.; Pang, M.; Cui, S.; Hou, Z.; Lin, J. A Multifunctional Cascade Bio reactor Based on Hollow-Structured Cu<sub>2</sub>MoS<sub>4</sub> for Synergetic Cancer Chemo-Dynamic Therapy/Starvation Therapy/Phototherapy/Immunotherapy with Remarkably Enhanced Efficacy. *Adv. Mater.* **2019**, *31*, 1905271. [[CrossRef](#)] [[PubMed](#)]

136. Li, S.; Shang, L.; Xu, B.; Wang, S.; Gu, K.; Wu, Q.; Sun, Y.; Zhang, Q.; Yang, H.; Zhang, F.; et al. A Nanozyme with Photo-Enhanced Dual Enzyme-Like Activities for Deep Pancreatic Cancer Therapy. *Angew. Chem. Int. Ed.* **2019**, *58*, 12624–12631. [[CrossRef](#)] [[PubMed](#)]
137. Zhao, Q.; Liu, J.; Deng, H.; Ma, R.; Liao, J.-Y.; Liang, H.; Hu, J.; Li, J.; Guo, Z.; Cai, J.; et al. Targeting Mitochondria-Located circRNA SCAR Alleviates NASH via Reducing mROS Output. *Cell* **2020**, *183*, 76–93. [[CrossRef](#)] [[PubMed](#)]
138. Feng, L.; Liu, B.; Xie, R.; Wang, D.; Qian, C.; Zhou, W.; Liu, J.; Jana, D.; Yang, P.; Zhao, Y. An Ultrasmall SnFe<sub>2</sub>O<sub>4</sub> Nanozyme with Endogenous Oxygen Generation and Glutathione Depletion for Synergistic Cancer Therapy. *Adv. Funct. Mater.* **2020**, *31*, 2006216. [[CrossRef](#)]